Suche nach Elektroweakinos mit dem ATLAS Detektor

Ludwig-Maximilians-Universität München
Fakultät für Physik

Dissertation

Eric Schanet

April 2021

Supervisor: PD Dr. Jeanette Lorenz

Part I

Fundamental concepts

Part II

The 1-lepton analysis

Part III

Reinterpretation

Chapter 11

Reinterpretation in the pMSSM

After having discussed to some extent efforts and methods to reinterpret ATLAS searches for Supersymmetry (SUSY), this chapter presents a reinterpretation of the 1-lepton analysis in the phenomenological Minimal Supersymmetric Standard Model (pMSSM). The truth analysis and simplified likelihoods discussed in chapters 9 and 10, respectively, are instrumental for the following sections.

11.1 Motivation

In today's searches for beyond the Standard Model (BSM) physics, it is common to use simplified models as a way of avoiding to necessity to deal with high-dimensional parameter spaces that are extremely challenging to sample and compare to data in an exhaustive way. The simplified model approach has also been used in the second part of this work, where results of the interpretation of the 1-lepton analysis in the $\tilde{\chi}_1^{\pm}\tilde{\chi}_2^0 \to Wh\tilde{\chi}_1^0\tilde{\chi}_1^0$ model have been presented. As has been discussed in section 1.2.7, simplified models are however by no means complete SUSY models and only serve as proxies for more complex and realistic SUSY scenarios. As such, simplified model limits cannot trivially be translated into limits on model parameters of a more complete SUSY model. Large-scale reinterpretations are necessary to understand the constraints today's SUSY searches set on realistic SUSY scenarios.

One class of more complete models, focussing on phenomenologically viable models, is the pMSSM, introduced in section 1.2.6. With its 19 parameters it offers much more complex SUSY scenarios while still being of somewhat manageable dimensionality. Still, large-scale reinterpretations in the pMSSM are computationally challenging and require a set of approximation as those introduced in chapters 9 and 10.

Large-scale reinterpretations in the pMSSM using a collection of relevant ATLAS SUSY searches not only allow to assess the sensitivity of the ATLAS SUSY search program towards more realistic SUSY scenarios, but can also potentially reveal interesting regions of the parameter space not yet covered by the current search programme. Moreover, such reinterpretations allow to demonstrate the sensitivity of simplified model searches beyond the simplified models they are originally interpreted in, thereby justifying the use of simplified models as proxies for more complete SUSY scenarios. In addition, reinterpretations in the pMSSM can be used to connect

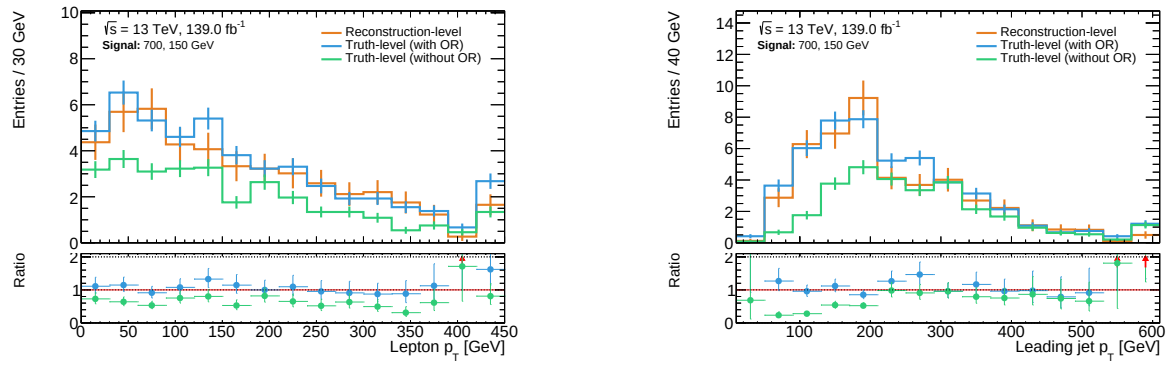

Figure 11.1: Impact of the overlap removal procedure at truth-level illustrated in the lepton and leading jet transverse momenta distributions. The truth-distribution without overlap removal (green) generally underestimates the number of signal events at reconstruction-level (orange). Correct overlap removal procedure at truth-level (blue) improves the agreement. The exemplary benchmark signal point with $m(\tilde{\chi}_1^{\pm}/\tilde{\chi}_2^0), m(\tilde{\chi}_1^0) = 700, 150\,\text{GeV}$ is shown in both plots (at truth- and reconstruction-level). All distributions are shown in a loose preselection requiring exactly one lepton, $E_{\text{T}}^{\text{miss}} > 50\,\text{GeV}$, $m_{\text{T}} > 50\,\text{GeV}$, and 2–3 jets, two of which need to be b-tagged.

the ATLAS SUSY searches with dark matter constraints from non-collider experiments, as well as Higgs and flavour measurements.

Although the following sections will be restricted to a reinterpretation of the 1-lepton search presented in the second part of this thesis, efforts are ongoing in ATLAS to perform large-scale reinterpretations using a majority of the full Run 2 ATLAS SUSY searches. These efforts will most likely result in one of the most comprehensive set of ATLAS constraints on SUSY yetope.

11.2 Truth-level analysis

As discussed in chapter 9, the reinterpretation of an analysis involves re-executing the analysis pipeline in order to derived signal rate estimates in all regions. In large-scale reinterpretations, running a RECAST implementation on all signal models considered is not computationally feasible and instead a *truth-level* analysis is first performed for all signal models sampled. Only models with uncertain exclusion at truth-level are processed through the computationally expensive full analysis chain implemented in RECAST. The truth-level analysis skips the detector simulation and uses generator-level objects instead. Any detector-level effects and inefficiencies will thus not be reflected in truth-level observables. In order to reproduce the kinematic distributions observed in the full analysis (using reconstruction-level objects), a dedicated *truth smearing*—discussed in detail in section 11.2.2—is applied.

11.2.1 Truth selection

All signal and control regions considered in the original 1-lepton search are implemented at truth-level using SIMPLEANALYSIS. The exact implementation is publicly available at Ref. [258]

and was already used in chapter 7 for the derivation of some of the theory uncertainties in the full analysis.

The truth-level implementation full specifies all object definitions introduced in section 4.4 even though some of them, like e.g. lepton isolation, are technically not well-defined at truth-level The subsequent smearing is in many cases implemented as a function of said object definitions and thus allows to consider them nonetheless. Additionally, as discussed in section 9.1, the full specification of the original analysis event selection including all object definitions allows for simpler reinterpretations by efforts outside of the ATLAS collaboration that generally do not have access to the original analysis software.

Following the object definitions, an overlap removal procedure following the same prescription as described for the reconstruction-level analysis is performed, i.e. especially also using the same shrinking cone definitions introduced in section 4.5. Overlap removal step removing electrons sharing a track with a muon is approximated by using a distance parameter of $\Delta R = 0.01$ between the objects. Although often neglected[†] in reinterpretation efforts outside of the collaboration, the correct implementation of the overlap removal procedure employed in the original analysis is typically crucial to reproduce the signal estimates of the original analysis, as illustrated in fig. 11.1. Furthermore, the exact implementation of all analysis observables is explicitly given in the SimpleAnalysis implementation, followed by the full definition of all control and signal regions.

11.2.2 Truth smearing

The general assumption of the truth smearing applied in the following is that the detector response roughly factorises into the responses of single particles. This allows to use detector performance results provided by ATLAS in order to construct detector response maps parameterised in different observables for each physics object. Detector response maps include object reconstruction and identification efficiencies as well as scale factors to correct for differences between Monte Carlo (MC) and observed data. Likewise, effects from the finite resolution of energy measurements in the detector are modelled through energy resolution maps. In the following, the 4-vector components of electrons, muons, jets and $E_{\mathrm{T}}^{\mathrm{miss}}$ are smeared. The implementation of the smearing functions is internal to ATLAS and originates predominantly from various upgrade studies.

In the case of truth electrons, the identifications efficiencies considered are parameterised in η and p_{T} as well as the identification working point used. In η, nine fixed-width bins are used. In p_{T}, six bins are implemented and a linear interpolation between two adjacent p_{T}-bins is used to get the efficiency for the given p_{T} of each truth electron. The probability of finding a fake electron in a truth jet is estimated through a similar two-dimensional map depending on the truth jet η and p_{T}, again using fixed-width bins in η and a linear interpolation in p_{T}. The range of the p_{T} interpolation for identification efficiencies and fake rates extends from 7 GeV to 120 GeV. If the truth p_{T} of the electron is outside of that range, the identification efficiency and fake rate from the respective bound of the corresponding η-bin are used. The probability for misidentifying an electron as a photon is estimated using different fixed values for the barrel

[†] The overlap removal procedures in ATLAS SUSY searches tend to be quite intricate, making them non-trivial to re-implement without ATLAS and analysis-specific knowledge.

and end-cap regions. Finally, the transverse energy of the electron is smeared using a random number drawn from a Gaussian distribution with standard deviation corresponding to the η- and p_{T}-dependent energy resolution.

For truth muons, the identification efficiencies are also parameterised in η and p_{T} as well as the identification working point used. Similar to truth electrons, the p_{T} of the muon is smeared using a Gaussian distribution with standard deviation corresponding to the momentum resolution. The momentum resolution of combined truth muons, σ_{CB}, is computed from the measured resolutions in the inner detector (ID),σ_{ID}, and muon spectrometer (MS), σ_{MS}, as

$$\sigma_{\mathrm{CB}} = \frac{\sigma_{\mathrm{ID}}\sigma_{\mathrm{MS}}}{\sqrt{\sigma_{\mathrm{ID}}^2 + \sigma_{\mathrm{MS}}^2}}, \tag{11.1}$$

where σ_{ID} and σ_{MS} are parameterised in η and p_{T}.

The transverse momentum of truth jets is smeared using a Gaussian with standard deviation equal to the jet energy resolution (JER), provided in a map parameterised in five bins in η ranging from $|\eta| = 0$ to $|\eta| = 4.5$. Following [216], jet energy resolutions are provided using parameterisations of a noise N, stochastic S and constant C term for each of the seven bins in $|\eta|$, such that the resolution can be computed as

$$\frac{\sigma(p_{\mathrm{T}})}{p_{\mathrm{T}}} = \frac{N}{p_{\mathrm{T}}} \oplus \frac{S}{\sqrt{p_{\mathrm{T}}}} \oplus C. \tag{11.2}$$

Only truth jets with $10\,\mathrm{GeV} < p_{\mathrm{T}} < 1.5\,\mathrm{TeV}$ are smeared. For truth jets with $p_{\mathrm{T}} > 20\,\mathrm{GeV}$, the flavour tagging efficiency is considered using efficiencies parameterised in η, p_{T} and the MV2c10 working point (introduced in section 4.4) used, measured in fully reconstructed simulated $t\bar{t}$ events [222].

Finally, the smeared missing transverse energy is computed using the transverse momenta of all smeared truth objects in the event, including an approximation for the track soft term. The latter is approximated using results from $Z \to e^+e^-$ events, allowing to infer a distribution of the mean soft term projected in the direction longitudinal to the total transverse momentum of all hard objects in an event, $\boldsymbol{p}_{\mathrm{T}}^{\mathrm{hard}}$. The measured resolution parallel and perpendicular to $\boldsymbol{p}_{\mathrm{T}}^{\mathrm{hard}}$ is then used to smear the nominal soft track value.

11.3 Validation of the truth-level analysis

11.3.1 Validation in loose preselection

The performance of the truth smearing is illustrated in a loose preselection for a single exemplary benchmark signal point in fig. 11.2. The loose preselection applied requires exactly one lepton, $E_{\mathrm{T}}^{\mathrm{miss}} > 50\,\mathrm{GeV}$, $m_{\mathrm{T}} > 50\,\mathrm{GeV}$, and 2–3 jets, two of which need to be b-tagged. The reconstruction-level distributions are compared with the truth-level distributions before and after truth smearing. It can clearly be observed that the truth smearing noticeably improves the agreement between the truth- and reconstruction-level distributions. While the lepton and jet reconstruction and identification efficiencies are—due to their dependence on η, p_{T}

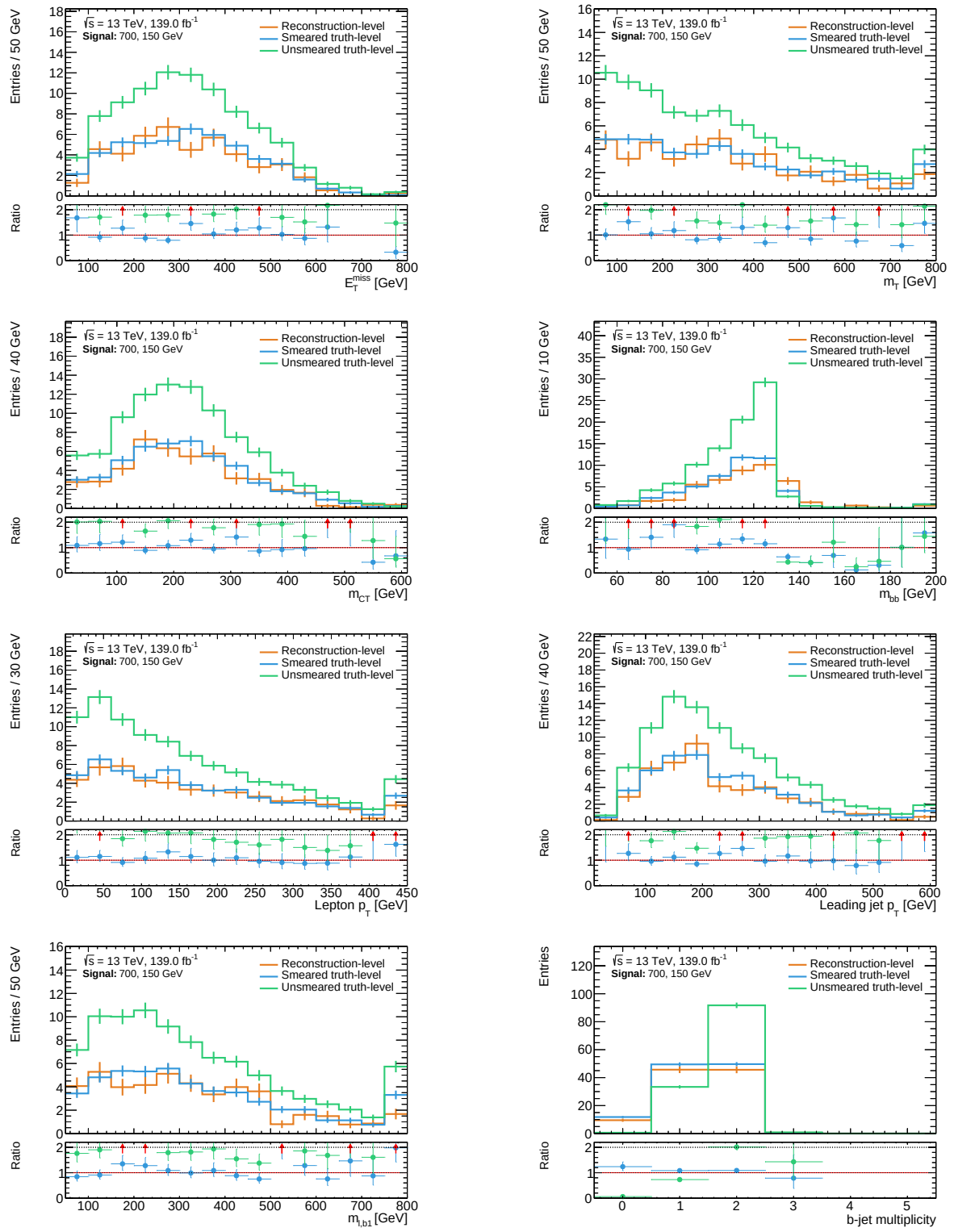

Figure 11.2: Comparisons of the kinematic distributions of key observables at (smeared) truth- and reconstruction-level. The exemplary benchmark signal point with $m(\tilde{\chi}_1^{\pm}/\tilde{\chi}_2^0), m(\tilde{\chi}_1^0) = 700, 150\,\text{GeV}$ is shown. The ratio pad shows the ratio between smeared and unsmeared truth-level distributions (blue and green) to reconstruction-level distributions (orange). Only MC statistical uncertainty is included in the error bars. All distributions are shown in a loose preselection requiring exactly one lepton, $E_{\text{T}}^{\text{miss}} > 50\,\text{GeV}$, $m_{\text{T}} > 50\,\text{GeV}$, and 2–3 jets, two of which need to be b-tagged. The latter requirement is dropped for the b-jet multiplicity distribution.

and individual working points—crucial for the overall agreement in shape, the inclusion of flavour-tagging efficiencies significantly improves the overall agreement in normalisation.

Although some minor differences remain, overall a good agreement is observed across all relevant kinematic distributions at loose preselection level. Most of the differences between smeared truth-level and reconstruction-level distributions in individual bins are well within the MC statistical uncertainties arising from the relatively limited MC statistics available.

11.3.2 Validation in signal regions

As the expected signal rates in the signal regions are ultimately what is entering the (simplified) likelihood, it is important that the good agreement observed at preselection is still present in the kinematically tighter selections of the signal regions. Additionally, it is worth investigating the agreement across all signal models considered in the original analysis, as opposed to only validating specific benchmark points. A comparison of the reconstruction-level and truth-level event rates before and after smearing in the signal regions SR-LM, SR-MM and SR-HM is shown in fig. 11.4 for all signal models considered in the 1-lepton analysis. For the sake of conciseness, only the cumulative m_{CT} bins are shown in each signal region (SR) in fig. 11.4. The agreement in the individual m_{CT} bins in each SR-LM, SR-MM and SR-HM is provided in figs. C.1 to C.3.

The truth smearing drastically improves the agreement in event rate estimates at truth- and reconstruction-level across all SR bins considered. While the event rates are generally overestimated at truth-level before smearing, compared to reconstruction-level, both tend to agree well within statistical uncertainties after smearing.

11.3.3 Validation using likelihood

Using the nominal expected event rates at smeared truth-level for every signal model in the original signal grid considered in the 1-lepton analysis, expected and observed CL_s values can be computed and exclusion contours can be derived. Figure 11.4(a) compares the expected and observed exclusion contours obtained using the full likelihood and reconstruction-level signal inputs with those obtained using the full likelihood and truth-level signal inputs before and after truth smearing. While all theory and systematic uncertainties on the signal are included in the reconstruction-level contours, no signal uncertainties are considered when obtaining both the smeared and unsmeared truth-level contours. As expected from the previous validation steps in the signal regions, the sensitivity using unsmeared truth-level signal inputs is significantly overestimated compared to the published analysis exclusion limit using reconstruction-level inputs. The smeared truth-level inputs, however, yield exclusion contours with an acceptable match compared to the reconstruction-level results.

With the truth smearing validated at multiple selection levels of the analysis, the full two-fold approximation of signal pipeline and statistical inference can be constructed. Figure 11.4(b) compares the exclusion contours of the original analysis results with those obtained using smeared truth-level signal inputs as well as the simplified likelihood. Even with the approximations made, overall a good agreement is found and the original analysis results can be reproduced to a relatively high degree of precision.

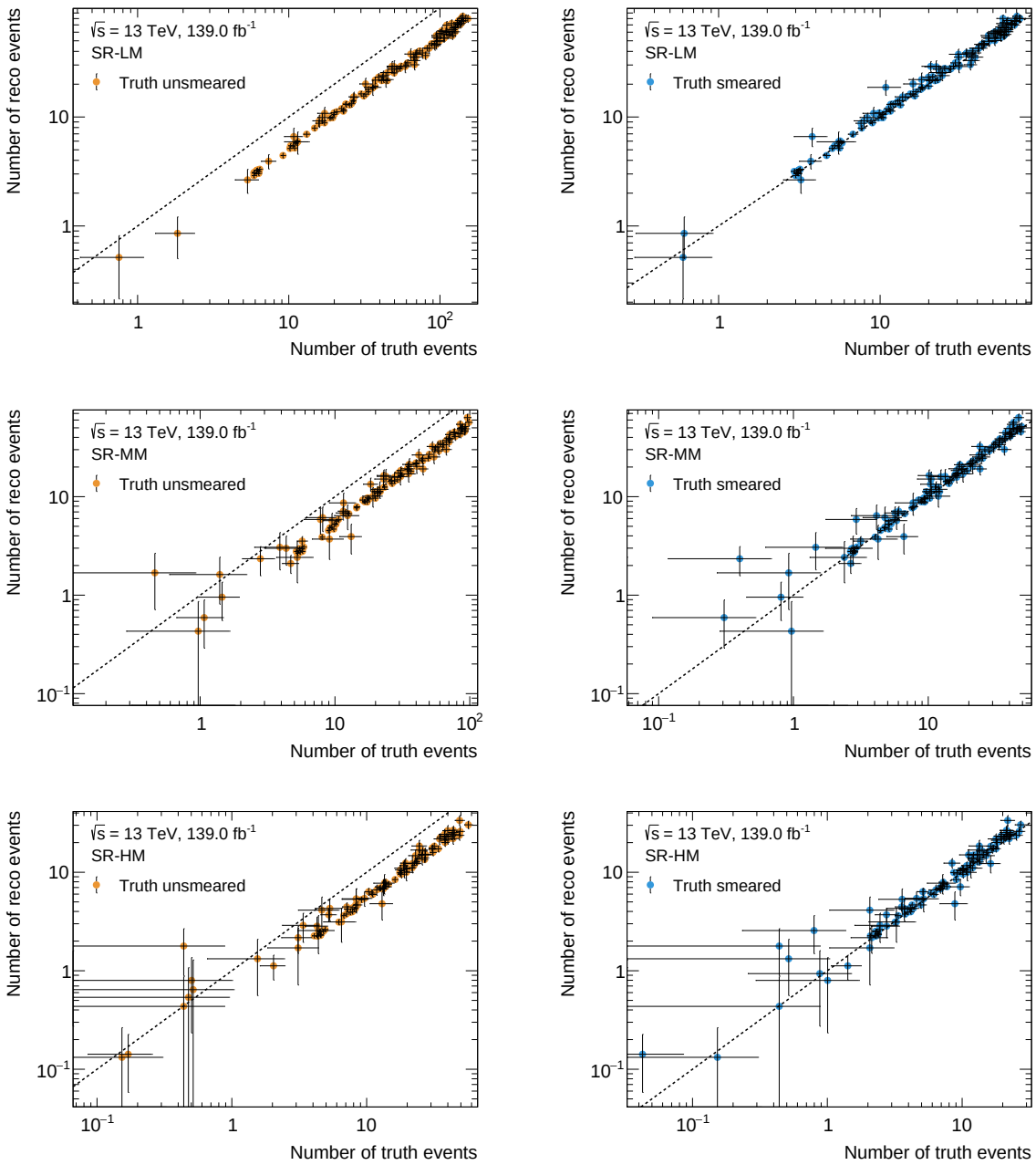

Figure 11.3: Comparison of the event rates at truth- and reconstruction-level before (left) and after (right) truth smearing. From top to bottom, the SR-LM, SR-MM and SR-HM signal regions are shown, with cumulative (integrated) m_{CT} bins. Every single point in the scatter plots represents a single signal model considered in the original 1-lepton analysis. Uncertainties include MC statistical uncertainties.

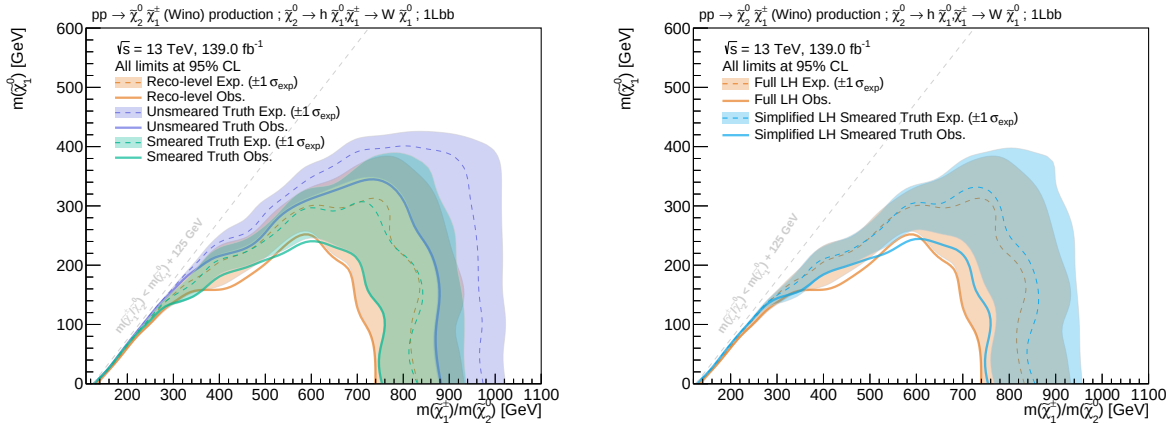

(a) **(b)**

Figure 11.4: Expected and observed exclusion contours obtained with the full and simplified likelihoods. Fig. (a) compares the full likelihood contours obtained with the reconstruction-level inputs (orange) to results obtained with truth inputs before (purple) and after (green) smearing. Fig. (b) compares the full likelihood reconstruction-level contours (orange) with those obtained using the simplified likelihood and smeared truth-level inputs (blue). Uncertainties include all statistical and systematic uncertainties on the background and signal for the reconstruction-level contours, but only statistical and systematic uncertainties on the background for truth-level signal inputs.

In summary, this validation process shows that the signal pipeline in fig. 9.1 can be efficiently approximated using truth-level analysis and a simplified treatment of the statistical model, allowing a considerably faster evaluation of BSM models while still offering reliable results. In large-scale reinterpretations, this approach thus enables an efficient classification of models into safely excluded and non-excluded models as well as models where exclusion is in doubt and where the full analysis pipeline using RECAST is needed.

11.4 Model sampling and processing

11.4.1 Sampling

All signal models considered in the following are sampled from the pMSSM using the parameter ranges shown in table 11.1. Flat probability distributions are used to draw random values within the given ranges for each parameter and each unique set of pMSSM parameters generated that way is referred to as an independent SUSY model.

As this work discusses a search for electroweakinos, the SUSY models drawn from the pMSSM are sampled with a special focus on said supersymmetric particles. This is achieved by setting the mass parameters of the first and second generation squarks as well as those of the sleptons to values much higher than those accessible at Large Hadron Collider (LHC) energies, effectively decoupling them. For naturalness arguments, third generation squarks and the gluino are not strictly decoupled but set to sufficiently high values such as not to affect the electroweak sector too much. The lower and upper bounds on the 12 scanned parameters are chosen to yield a high density of models with electroweakino masses accessible at LHC energies.

Table 11.1: Scan ranges used for each of the 19 pMSSM parameters. For parameters written with a modulus sign, both the positive and negative values are allowed. The term "gen(s)" refers to generation(s).

Parameter	min	max	Note
$m_{\tilde{L}_1}$ $(= m_{\tilde{L}_2})$	10 TeV	10 TeV	Left-handed slepton (first two gens.) mass
$m_{\tilde{e}_1}$ $(= m_{\tilde{e}_2})$	10 TeV	10 TeV	Right-handed slepton (first two gens.) mass
$m_{\tilde{L}_3}$	10 TeV	10 TeV	Left-handed stau doublet mass
$m_{\tilde{e}_3}$	10 TeV	10 TeV	Right-handed stau mass
$m_{\tilde{Q}_1}$ $(= m_{\tilde{Q}_2})$	10 TeV	10 TeV	Left-handed squark (first two gens.) mass
$m_{\tilde{u}_1}$ $(= m_{\tilde{u}_2})$	10 TeV	10 TeV	Right-handed up-type squark (first two gens.) mass
$m_{\tilde{d}_1}$ $(= m_{\tilde{d}_2})$	10 TeV	10 TeV	Right-handed down-type squark (first two gens.) mass
$m_{\tilde{Q}_3}$	2 TeV	5 TeV	Left-handed squark (third gen.) mass
$m_{\tilde{u}_3}$	2 TeV	5 TeV	Right-handed top squark mass
$m_{\tilde{d}_3}$	2 TeV	5 TeV	Right-handed bottom squark mass
$\lvert M_1 \rvert$	0 TeV	2 TeV	Bino mass parameter
$\lvert M_2 \rvert$	0 TeV	2 TeV	Wino mass parameter
$\lvert \mu \rvert$	0 TeV	2 TeV	Bilinear Higgs mass parameter
M_3	1 TeV	5 TeV	Gluino mass parameter
$\lvert A_t \rvert$	0 TeV	8 TeV	Trilinear top coupling
$\lvert A_b \rvert$	0 TeV	2 TeV	Trilinear bottom coupling
$\lvert A_\tau \rvert$	0 TeV	2 TeV	Trilinear τ lepton coupling
M_A	0 TeV	5 TeV	Pseudoscalar Higgs boson mass
$\tan\beta$	1	60	Ratio of the Higgs vacuum expectation values

Once a value for each of the 19 pMSSM parameters has been chosen, a number of publicly available software packages are executed in order to compute the properties of each model point. In a first step, SPheno v4.0.5 [274, 275] is used to calculate the spectrum of the sparticles. The result of SPheno is used to determine the masses and mixings of the Higgs bosons using FeynHiggs v2.15.0 [276–278]. An additional SUSY spectrum calculation is performed with SoftSusy v4.1.8 [279]. Although the masses, mixings and branching fractions from SoftSusy will not directly be used in the following, the program is still required to complete successfully in order to reduce the number of pMSSM models with pathological properties. After the complete model spectrum has calculated, additional properties are determined. The dark matter relic abundance of each model is calculated with micrOMEGAs v5.0.8 [280, 281]. Finally, flavour physics and precision electroweak observables like $\Delta\rho$, $\Delta(g-2)_\mu$, $\mathrm{BR}(b \to s\gamma)$ and $\mathrm{BR}(B_s \to \mu^+\mu^-)$ are determined using SuperIso v4.0 [282].

11.4.2 Selection and processing

In order to avoid models with pathological properties, all spectrum generators are required to finish execution without error. The cross section for surviving models is computed at next-to-leading order (NLO) using Prospino v2.1 [283, 284]. Models with an inclusive cross sections for all electroweak production processes below 0.07 fb are discarded as they would result in less than 10 expected signal events with an integrated luminosity of 139 fb^{-1}, not enough to be sensitive to with current electroweak SUSY searches. Finally, models with long-lived or even

stable (on the time scale needed for traversing the ATLAS detector) sparticles[†] are discarded as SUSY searches targeting prompt electroweakino decays (like the 1-lepton search), are not expected to be sensitive to these models.

No constraints on the computed cosmological LSP abundance and precision electroweak and flavour observables are applied at this stage in order to give a more general view after the models are evaluated using the 1ℓ search. Experimental constraints from e.g. Large Electron Positron (LEP) are also not applied at this stage.

Of the 10,000 unique models sampled from the pMSSM using the above prescription, 5152 models survive the constraints and requirements discussed in this section and are analysed using the 1ℓ search. The majority of the models rejected due to the cross section constraints.

11.4.3 Event generation

Event generation is performed using the software centrally provided by the ATLAS production system. The initial pair of sparticles with two one parton in the matrix element (ME) are generated using the MadGraph5_aMC@NLO v2.6.1. [175, 176] generator. Next, Pythia8.230 [177] with the A14 tune is used for the hadronisation and parton shower (PS), together with the NNPDF 2.3 LO [179] parton distribution function (PDF) set. The number of events generated scales with the cross section of the model, starting at 10^4 and capping out at 10^6 truth-level events.

11.4.4 Truth-level analysis

All models passing event generation are evaluated using the truth-level analysis described in section 11.2. This is the only evaluation done for the models considered in this work. A full scan over the pMSSM including multiple ATLAS SUSY searches would most likely include an additional processing step reverting to reconstruction-level analysis including the original analysis pipelines and full detector reconstruction for model points where (non-)exclusion is uncertain based on truth-level analysis only.

11.5 Phenomenology of the LSP

The composition of the $\tilde{\chi}_1^0$ in each pMSSM model sampled is shown in the $m(\tilde{\chi}_1^\pm)$–$m(\tilde{\chi}_1^0)$ and $m(\tilde{\chi}_2^0)$–$m(\tilde{\chi}_1^0)$ plane in figs. 11.5(a) and 11.5(b), respectively. The $\tilde{\chi}_1^0$ is considered to be bino-like ($\tilde{B}$-like), wino-like ($\tilde{W}$-like) or higgsino-like ($\tilde{H}$-like) if the corresponding fraction from the neutralino mass mixing matrix is at least 80%. If more than one component has a fraction of more than 20%, then the $\tilde{\chi}_1^0$ is considered to be of mixed nature.

In the bulk of the $m(\tilde{\chi}_1^\pm)$–$m(\tilde{\chi}_1^0)$ plane, i.e. the parameter space targeted by the 1ℓ search using the simplified model, the large majority of the models produce a bino-like LSP with nearly mass-degenerate $\tilde{\chi}_1^\pm$ and $\tilde{\chi}_2^0$. These models correspond to cases where $M_1 \ll M_2, \mu$ and are closest to the canonical simplified model considered in the 1ℓ search. Some sensitivity can be

[†] Not considering the lightest supersymmetric particle (LSP).

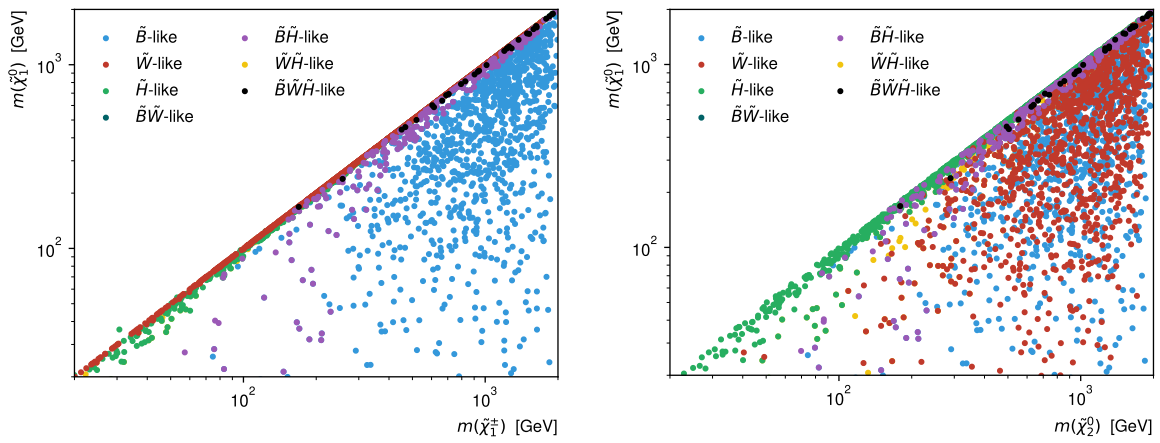

(a) **(b)**

Figure 11.5: Scatter plot of all models sampled in the (a) $m(\tilde{\chi}_1^\pm)$–$m(\tilde{\chi}_1^0)$ and (b) $m(\tilde{\chi}_2^0)$–$m(\tilde{\chi}_1^0)$ planes. The colour encodes the composition of the $\tilde{\chi}_1^0$ in each model. The $\tilde{\chi}_1^0$ is considered to be bino-like ($\tilde{B}$-like), wino-like ($\tilde{W}$-like) or higgsino-like ($\tilde{H}$-like) if the corresponding fraction from the neutralino mass mixing matrix is at least 80%. Additionally, the $\tilde{\chi}_1^0$ is considered to be of mixed nature if more than one component has a fraction of 20%. For example, a $\tilde{B}\tilde{W}$-like $\tilde{\chi}_1^0$ has more than 20% bino and wino components, but less than 20% higgsino component.

expected towards these models using the 1ℓ search, provided that the branching fractions of the decays $\tilde{\chi}_1^\pm \to W^\pm\tilde{\chi}_1^0$ and especially $\tilde{\chi}_2^0 \to h\tilde{\chi}_1^0$ are large enough and produce on-shell bosons.

Towards the diagonal of $m(\tilde{\chi}_1^\pm)$–$m(\tilde{\chi}_1^0)$ plane, i.e. for models where the $\tilde{\chi}_1^\pm$ and $\tilde{\chi}_1^0$ are nearly mass-degenerate, the nature of the LSP shows a larger variation. In a large set of models, the LSP has a significant wino component, leading to a mass spectrum where the $\tilde{\chi}_1^\pm$ and $\tilde{\chi}_1^0$ are nearly mass-degenerate while the mass of the $\tilde{\chi}_2^0$ can take on higher values. In models where the LSP has a large higgsino component, i.e. $\mu \ll M_1, M_2$, all three sparticles ($\tilde{\chi}_1^\pm$, $\tilde{\chi}_2^0$ and $\tilde{\chi}_1^0$) are nearly mass-degenerate and result in very soft decay products, making these models inherently difficult to target.

11.6 Impact of the 1-lepton search on the pMSSM

The impact of the 1-lepton search on the pMSSM is discussed using one-dimensional and two-dimensional distributions in the following sections. As usual, a model is considered to be excluded if the observed CL_s value obtained from the simplified likelihood using the smeared truth-level inputs is below 0.05. Of the 7264 models evaluated, the 1ℓ search excludes a total of 98, or about 1.3%, of the models.

For the one-dimensional distributions shown in the following, the total number of models is compared against the number of models excluded by the 1ℓ search. An additional pad indicates the ratio between models excluded and total models sampled in each bin of the distribution. In the two-dimensional distributions, the numbers in the bins indicate the number of pMSSM

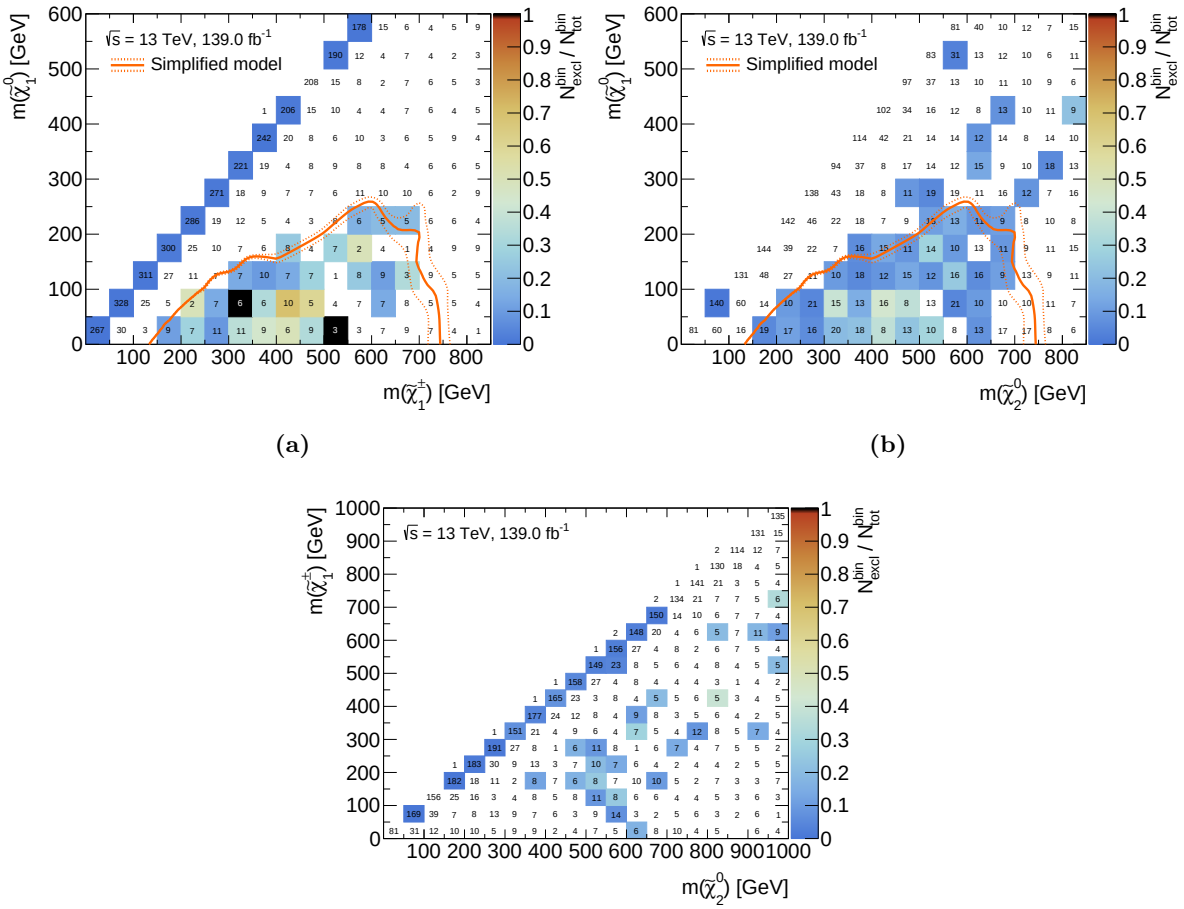

Figure 11.6: Bin-by-bin fraction of excluded models as a function of the relevant sparticle masses. The numbers in the bins correspond to the total number of models sampled falling into the respective bin. The number of models excluded by the 1-lepton analysis is encoded with a colour bar ranging from 0 to 1. Where all models in a given bin are excluded, the bin is coloured in black. Bins without any models excluded are left white. Models are evaluated using the simplified likelihood of the 1-lepton analysis. The simplified model contour is shown in orange.

models falling into each respective bin. In these distributions, the fraction of models excluded with the 1ℓ search is encoded using the z-axis, represented by a colour bar.

11.6.1 Impact on electroweakino masses

Figures 11.6 and 11.7 show the bin-by-bin fractions of models excluded by the 1ℓ search as two- and one-dimensional distributions, respectively. From the $\tilde{\chi}_1^{\pm}$–$\tilde{\chi}_1^0$ plane in fig. 11.6(a), it can be seen that the 1ℓ search is most sensitive to pMSSM models in mass ranges similar to those excluded in the context of the simplified model. Most of the models excluded have $\tilde{\chi}_1^{\pm}/\tilde{\chi}_2^0$ masses ranging from roughly 200 GeV to about 700 GeV and LSP ranging masses from 0 GeV

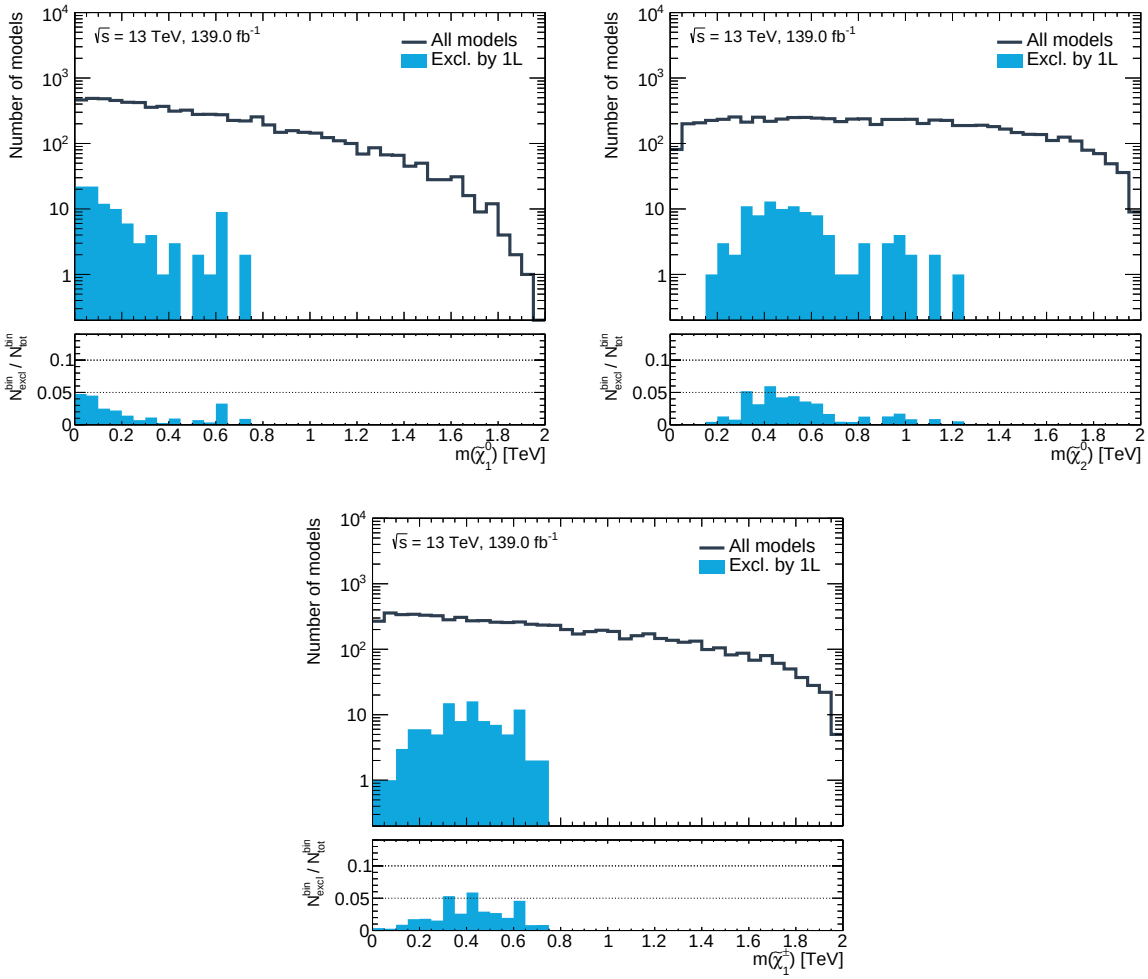
Number of models
√s = 13 TeV, 139.0 fb-1
All models
Excl. by 1L
N_excl^bin / N_tot^bin
m(χ̃1^0) [TeV]
m(χ̃2^0) [TeV]
m(χ̃1^±) [TeV]

Figure 11.7

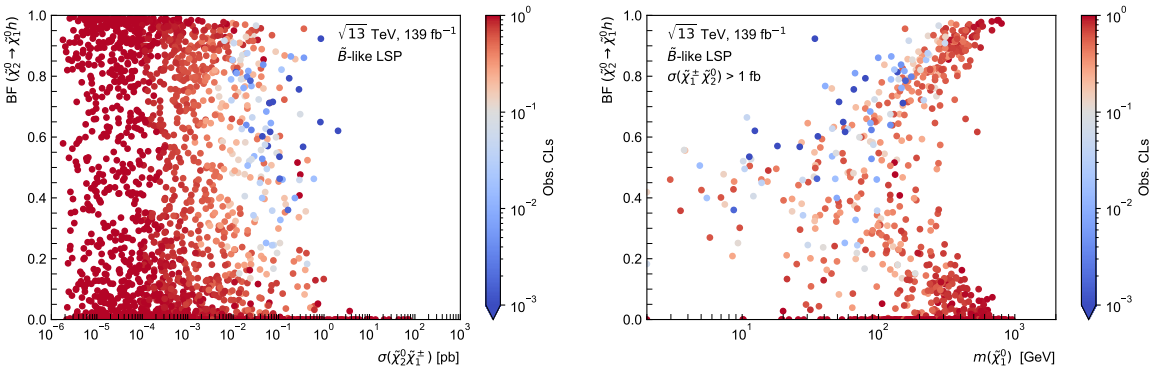

(a) **(b)**

Figure 11.8

to about 300 GeV. The proportion of excluded models peaks at $m(\tilde{\chi}_1^\pm, \tilde{\chi}_2^0) \approx 450$ GeV and light LSPs with $\tilde{\chi}_1^0 < 150$ GeV, as visible in fig. 11.7.

The models excluded by the 1ℓ search can roughly be classified in two categories: models lying within the simplified model exclusion contour and models with nearly mass-degenerate $\tilde{\chi}_1^\pm$ and $\tilde{\chi}_2^0$. As discussed in section 11.5, most models within the simplified model exclusion contour produce a bino-like LSP and result in nearly mass-degenerate $\tilde{\chi}_1^\pm$ and $\tilde{\chi}_2^0$. Figure C.4 illustrates this behaviour further. Expectedly, the 1ℓ search is thus most sensitive to $\tilde{\chi}_1^\pm\tilde{\chi}_2^0$ production with wino-like electroweakinos and a bino-like $\tilde{\chi}_1^0$, corresponding to models with a spectrum close to that of the canonical simplified model signature originally considered in the search.

The second category of models excluded comprises cases where the LSP is wino-like and nearly mass-degenerate with the $\tilde{\chi}_1^\pm$, corresponding to the diagonal in fig. 11.6(a) As the mass difference between the LSP and the $\tilde{\chi}_1^\pm$ is typically much smaller than the W boson mass, the $\tilde{\chi}_1^\pm$-decay primarily proceeds through off-shell W bosons, $\tilde{\chi}_1^\pm \to W^*\tilde{\chi}_1^0$, resulting in soft leptons that often cannot be reconstructed in the analysis. Even though no sensitivity to these models is expected from the 1ℓ search, a small set of models with a wino-like LSP can still be excluded. These correspond to cases where the $\tilde{\chi}_2^\pm$ is not too heavy such that the 1ℓ search is sensitive to $\tilde{\chi}_2^\pm\tilde{\chi}_2^0$ production with cross sections of $\mathcal{O}(1\,\text{fb})$. If the $\tilde{\chi}_2^\pm$ decays directly into the LSP via $\tilde{\chi}_2^\pm \to W^\pm\tilde{\chi}_1^0$, enough events with an isolated lepton can occur, allowing to exclude the model. (see e.g. fig. C.5(c)).

No sensitivity is observed for pMSSM models with higgsino-like electroweakinos and thus compressed mass spectra. This is expected, as such scenarios typically produce off-shell W, Z and h bosons, resulting in very soft final state objects the 1ℓ search is not optimised for. Dedicated searches (see e.g. Ref. [270]) exist in ATLAS to target such compressed scenarios and work is ongoing to include these in the scans of the pMSSM.

In general, the sensitivity to pMSSM models is significantly reduced compared to the simplified model exclusion contour, even in the parameter space generating models similar to the simplified model. The crucial difference, responsible for the loss in sensitivity, is the fact that the simplified model assumes branching ratios of 100% of the $\tilde{\chi}_1^\pm \to W^\pm\tilde{\chi}_1^0$ and $\tilde{\chi}_2^0 \to h\tilde{\chi}_1^0$ decays. While the former is in general a good assumption in pMSSM models where $m(\tilde{\chi}_1^\pm) \lesssim m(\tilde{\chi}_2^0)$, the latter

often is not the dominant decay of the $\tilde{\chi}_2^0$ which may decay through $\tilde{\chi}_2^0 \to Z\tilde{\chi}_1^0$ instead. The couplings of the $\tilde{\chi}_2^0$ to the Higgs boson are suppressed by powers of $|\mu|/M_2$ in the gaugino-like regions [285], meaning that the branching fraction of $\tilde{\chi}_2^0 \to h\tilde{\chi}_1^0$ takes on reasonably high values only in models with an LSP containing a substantial bino component. The Higgs coupling suppression is illustrated in fig. C.7. As can be seen from fig. 11.6(a), even in the bulk of the $\tilde{\chi}_1^\pm$–$\tilde{\chi}_1^0$ plane—containing mostly models with a bino-like LSP—not all models can be excluded by the 1ℓ search. Figure 11.8(a) shows that many of these models have either a too small $\tilde{\chi}_1^\pm\tilde{\chi}_2^0$ pair-production cross section or too low values for $\mathrm{BF}(\tilde{\chi}_2^0 \to h\tilde{\chi}_1^0)$. For the few non-excluded models with reasonable $\tilde{\chi}_1^\pm\tilde{\chi}_2^0$ pair-production cross section ($> \mathcal{O}(1\,\mathrm{fb})$) and high enough Higgs coupling to $\tilde{\chi}_2^0$, the mass of the LSP turns out to be too high (see fig. 11.8(b)), typically resulting in final states with insufficient $E_\mathrm{T}^\mathrm{miss}$ and soft objects.

As a cross-check, a significant portion of the models with bino-like LSP were reprocessed with $\mathrm{BF}(\tilde{\chi}_2^0 \to h\tilde{\chi}_1^0)$ fixed to unity and subsequently analysed with the 1ℓ search. The results can be seen in Figure C.8(b), revealing that significantly more models can be excluded within the simplified model contour when the simplified model branching fraction assumption is restored. As the $\tilde{\chi}_2^0$ decay into a Z boson and $\tilde{\chi}_1^0$ is the competing decay to $\tilde{\chi}_2^0 \to h\tilde{\chi}_1^0$, combining searches targeting these decay modes could recover the loss in sensitivity. Likewise, the development of searches targeting both decay modes at the same time would also recover the full sensitivity[†].

11.6.2 Impact on pMSSM parameters

The impact of the 1ℓ search on the pMSSM parameters relevant to the electroweak sector are shown in one-dimensional distributions in fig. 11.9. As already discussed in section 11.6.1, the 1ℓ search has the largest impact for small values in the bino mass parameter M_1, leading to models with a bino-like LSP when $M_1 \ll M_2 \lesssim \mu$. Consequently, the proportion of excluded models peaks at slightly higher values in the distribution of the wino mass parameter, $|M_2| \approx 400\,\mathrm{GeV}$. As the search is not sensitive to compressed scenarios with a higgsino-like LSP, no models with small values in $|\mu|$ can be excluded.

As the pseudoscalar Higgs boson does not directly enter the phenomenology of the models targeted by the 1ℓ search, only indirect constraints are provided on m_A, excluding models in the full range of the m_A distribution sampled. A similar behaviour is observed in $\tan\beta$ where the excluded models have values of $\tan\beta$ spanning the full range from 1 to 60. Likewise, no direct constraints on the trilinear scalar couplings (A_t, A_b, A_τ), and the remaining gluino and third generation squark mass parameters (M_3, $m_{\tilde{Q}_3}$, $m_{\tilde{u}_3}$, $m_{\tilde{d}_3}$) is observed. As can be seen from fig. C.9, the 1ℓ search excludes values of these parameters across the entire range originally sampled.

11.6.3 Impact on dark matter relic density

The $\tilde{\chi}_1^0$ cosmological abundance in dependence of its type and mass is shown in fig. C.10(a). The measurement of the dark matter (DM) relic density by the Planck mission is shown as dashed line and interpreted as upper limit on the DM relic density, allowing the $\tilde{\chi}_1^0$ to be a sub-dominant DM component. Some interesting features can be highlighted. First, most

[†] Provided that they are targeted with disjoint signal regions such that a combined likelihood can be built.

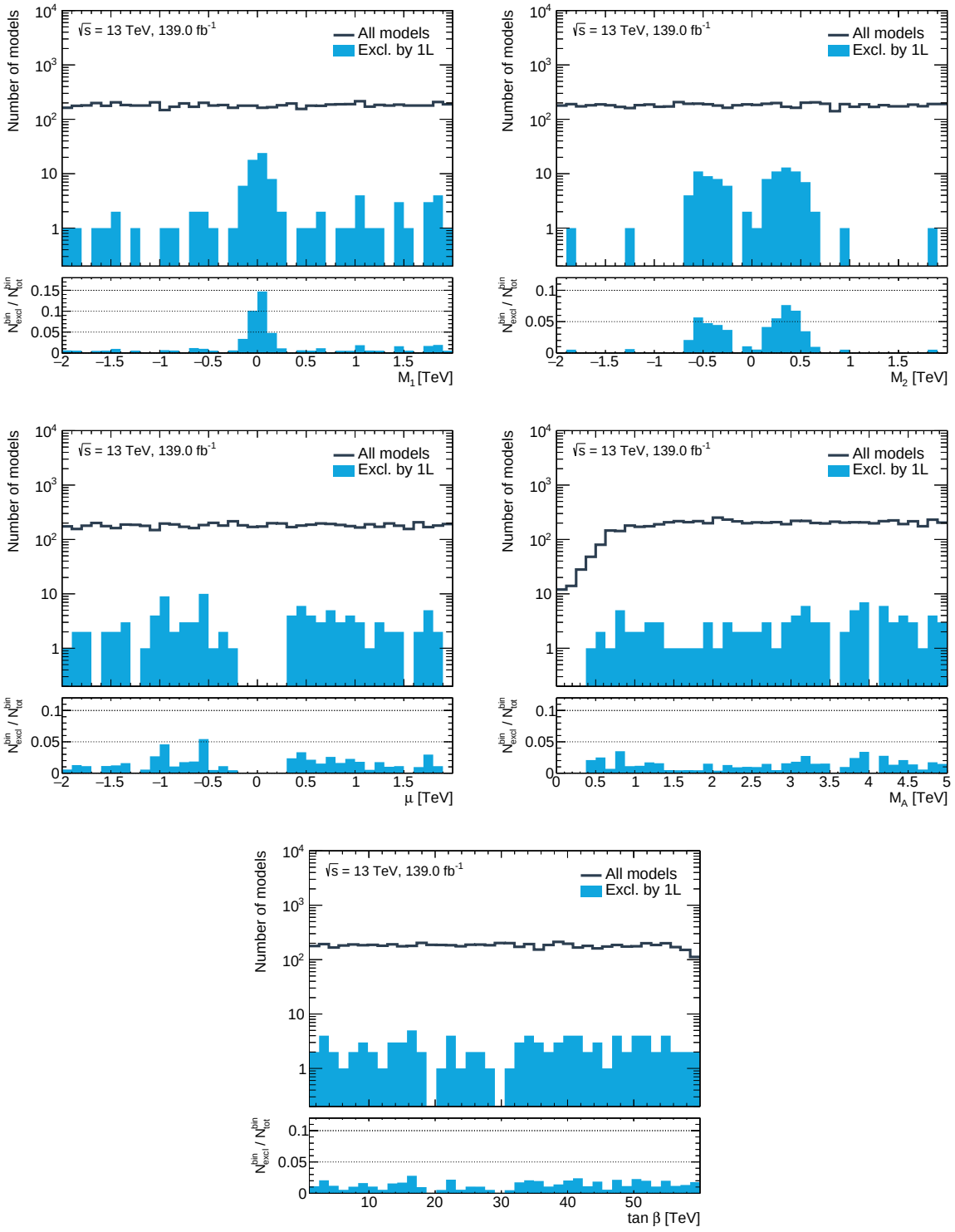
√s = 13 TeV, 139.0 fb-1
All models
Excl. by 1L
Number of models
M1 [TeV]
M2 [TeV]
μ [TeV]
MA [TeV]
tan β [TeV]

Figure 11.9

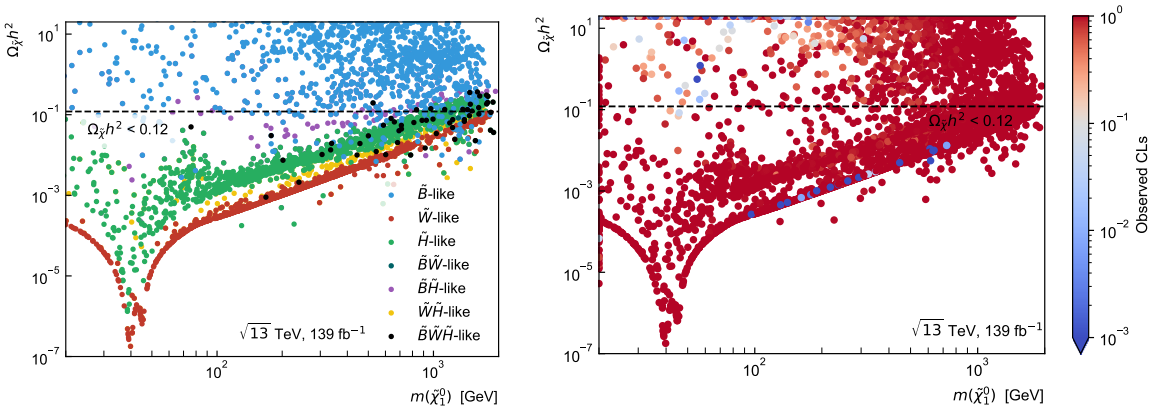

(a) **(b)**

Figure 11.10

of the models sampled with bino-like $\tilde{\chi}_1^0$ result in a cosmological abundance $\Omega_{\tilde{\chi}}h^2 > 0.12$ incompatible with the result from Planck. Of the pMSSM models sampled in this work, only models containing a $\tilde{\chi}_1^0$ with a considerable wino or higgsino component satisfy $\Omega_{\tilde{\chi}}h^2 < 0.12$ over a large range of $m(\tilde{\chi}_1^0)$. Models with $m(\tilde{\chi}_1^0) \simeq m(Z)/2$ produce especially low values in $\Omega_{\tilde{\chi}}h^2$ as the $\tilde{\chi}_1^0$ can resonantly annihilate through s-channel Z exchange. This is the so-called *Z-funnel* [286]. A similar funnel exists around $m(h)/2$ but is not visible in fig. C.10(a) due to an additional resonant process: co-annihilation of a nearly mass-degenerate $\tilde{\chi}_1^\pm\tilde{\chi}_1^0$ pair at $m(W)/2$ through s-channel W exchange.

In practice, experimental constraints like e.g. the LEP limit of $m(\tilde{\chi}_1^\pm) \gtrsim 100\,\text{GeV}$ (the actual limit depends on the exact configuration of the SUSY mass spectrum probed) rule out models with $|M_2|, |\mu| \lesssim 100\,\text{GeV}$. The effect of this in the $\Omega_{\tilde{\chi}}h^2$–$m(\tilde{\chi}_1^0)$ plane is shown in fig. C.10, revaealing that models containing a $\tilde{\chi}_1^0$ with a large wino or higgsino component and $m(\tilde{\chi}_1^0) \lesssim 100\,\text{GeV}$ are largely ruled out, leaving models with a bino-like $\tilde{\chi}_1^0$ as the only remaining possibility in this region. Although theoretically models with a bino-like $\tilde{\chi}_1^0$ could produce low $\tilde{\chi}_1^0$ relic density values through the Z- and h-funnels, in practice they are not sampled in this work due to the limited number of bino-like $\tilde{\chi}_1^0$ models sampled in combination with relative accumulation at large $\tilde{\chi}_1^0$ masses of models with a bino-like $\tilde{\chi}_1^0$. For this reason, in this work, only a very small number of models with a bino-like $\tilde{\chi}_1^0$ with $m(\tilde{\chi}_1^0) \lesssim 100\,\text{GeV}$ have a relic density compatible with the Planck measurement. Oversampling this region in the parameter space still reveals the Z- and h-funnels for models with a bino-like $\tilde{\chi}_1^0$, as can be seen in e.g. Refs. [76, 75]. If the $\tilde{\chi}_1^\pm/\tilde{\chi}_2^0$ masses of such models fall into the range where the 1ℓ search is sensitive,i.e. $\tilde{\chi}_1^\pm\tilde{\chi}_2^0$ pair-production has high enough cross section, the 1ℓ search can be excepted to exclude a large fraction of these models, warranting additional studies and dedicated pMSSM scans using experimental constraints in the sampling priors.

Although of limited use due to the reasons just discussed, the impact of the 1ℓ search on the DM relic density can still be investigated with the models available. Figure 11.10(b) shows the $\tilde{\chi}_1^0$ cosmological abundance in dependence of its mass. Instead of encoding the nature of the $\tilde{\chi}_1^0$, the colour now encodes the observed CL_s value obtained by the 1ℓ search. By comparing with fig. C.10(a) it can be seen that the majority of the models with a bino-like $\tilde{\chi}_1^0$ excluded by

the 1ℓ search have a cosmological abundance not satisfying $\Omega_{\tilde{\chi}}h^2 < 0.12$. Through its limited sensitivity to some of the models with a wino-like $\tilde{\chi}_1^0$, the 1ℓ search is however still able to constrain $\Omega_{\tilde{\chi}}h^2$, even if only for a few select models.

11.7 Discussion

Large-scale reinterpretations in high-dimensional SUSY model spaces are crucial in order to assess the sensitivity of SUSY searches in the context of realistic SUSY scenarios. The evaluation of signal models at smeared truth level in combination with the simplified likelihoods introduced in chapter 10 offers a computationally efficient but still reliable approach for such reinterpretations.

A reinterpretation of the 1ℓ search in a limited number of models sampled from the pMSSM with a focus on the electroweak sector revealed that the search is sensitive to SUSY beyond the simplified model originally considered. In general, the simplified model phenomenology maps reasonably well onto a portion of the pMSSM parameter space. The sensitivity of the 1ℓ search towards pMSSM models is however negatively impacted by the competing decays $\tilde{\chi}_2^0 \to Z\tilde{\chi}_1^0$ and $\tilde{\chi}_2^0 \to h\tilde{\chi}_1^0$, a circumstance that breaks one of the main assumptions of the simplified model. In order to maximise the sensitivity of future searches to $\tilde{\chi}_1^\pm\tilde{\chi}_2^0$ pair-production in more complete SUSY scenarios, it is crucial to target both decay modes at the same time. In searches targeting final states with one lepton, multiple jets and missing transverse momentum, both the b-jet multiplicity as well as the invariant mass of the jets originating from the decays $h \to b\bar{b}$ and $Z \to q\bar{q}$ can easily be used to construct disjoint[†] signal regions targeting both decay modes.

Going even further than this, it would be worth targeting not only $\tilde{\chi}_1^\pm\tilde{\chi}_2^0$ production, but also $\tilde{\chi}_1^\pm\tilde{\chi}_1^\pm$ production at the same time through a single likelihood. In ATLAS, work is ongoing to perform a e.g. a 1ℓ search with dedicated signal regions targeting both $\tilde{\chi}_1^\pm\tilde{\chi}_2^0 \to WZ\tilde{\chi}_1^0\tilde{\chi}_1^0 \to \ell\nu_\ell q\bar{q}\tilde{\chi}_1^0\tilde{\chi}_1^0$ and $\tilde{\chi}_1^\pm\tilde{\chi}_1^\pm \to WW\tilde{\chi}_1^0\tilde{\chi}_1^0 \to \ell\nu_\ell q\bar{q}'\tilde{\chi}_1^0\tilde{\chi}_1^0$ at the same time.

Finally, the impact of the 1ℓ search on the DM relic density was discussed. Due to the parameter ranges chosen during sampling and the lack of experimental constraints applied, many models sampled are not directly relevant to the DM phenomenology. Only a small number of models with a bino-like $\tilde{\chi}_1^0$ are sampled in the Z- and h-funnel region where $\Omega_{\tilde{\chi}}h^2 < 0.12$ is satisfied. Outside of these two funnels, models with a bino-like $\tilde{\chi}_1^0$ only satisfy the relic density constraint for $\tilde{\chi}_1^\pm$ and $\tilde{\chi}_1^0$ masses outside of the parameter space the 1ℓ search is sensitive to. In order to be able to further investigate the impact of the 1ℓ search on DM observables—especially in the Z and h-funnels—a different sampling technique would need to be adopted and models with bino-like $\tilde{\chi}_1^0$ need to be oversampled in the relevant region of the parameter space.

[†] Building signal regions that are not orthogonal to each other prevents the construction of a single likelihood and thus does not allow to fit all regions simultaneously.

Part IV

Summary and Outlook

Part V

Appendix

Appendix C

C.1 Truth smearing

C.2 Impact of LSP type

C.3 Higgs coupling to neutralinos

C.4 Impact of mixed branching fractions

C.5 Impact on pMSSM parameters

C.6 Impact on dark matter relic density

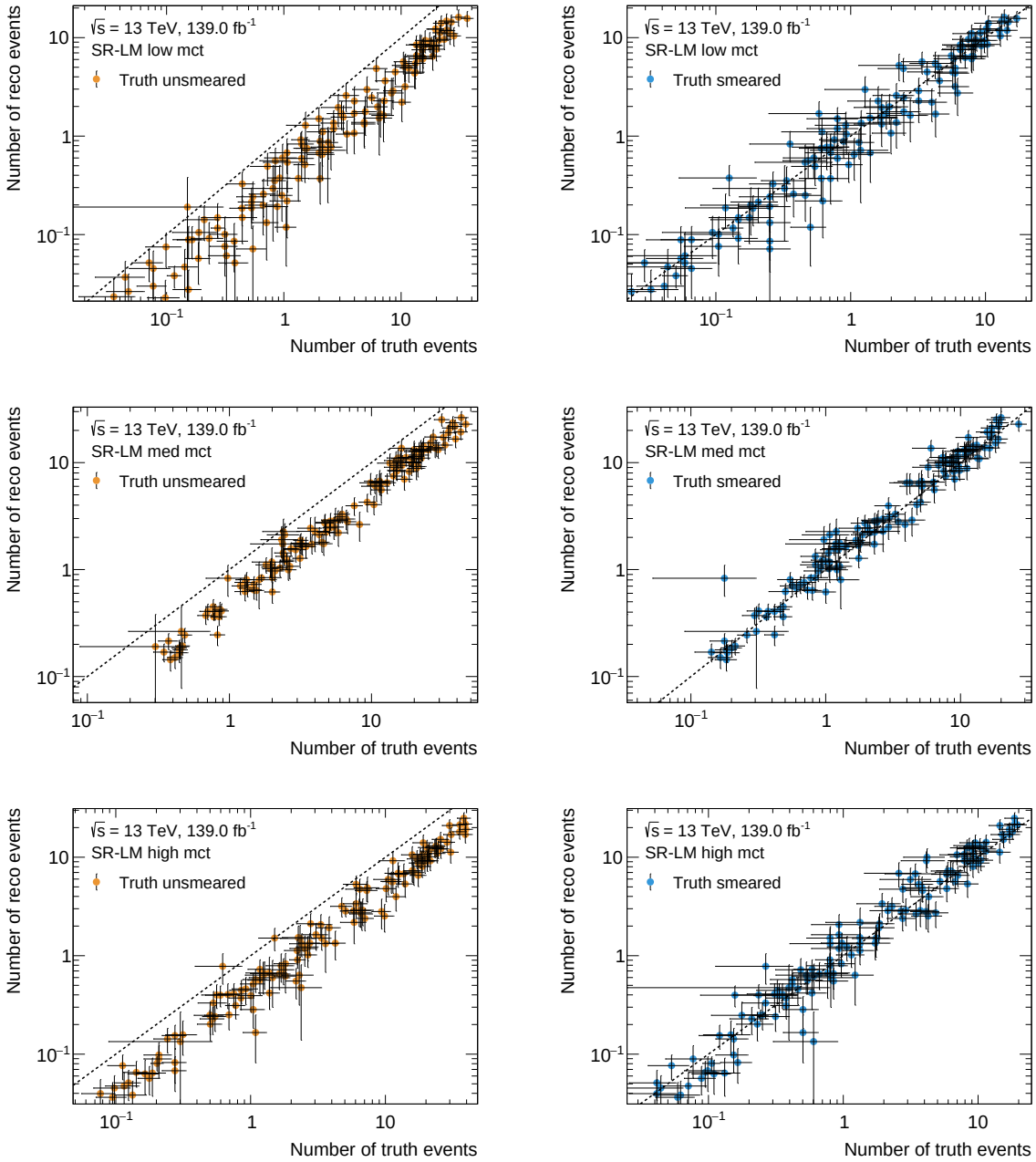

Figure C.1: Comparison of the event rates at truth- and reconstruction-level before (left) and after (right) truth smearing in SR-LM. From top to bottom, the low, medium and high m_{CT} bins are shown. Every single point in the scatter plots represents a single signal model considered in the original 1-lepton analysis. Uncertainties include only MC statistical uncertainties.

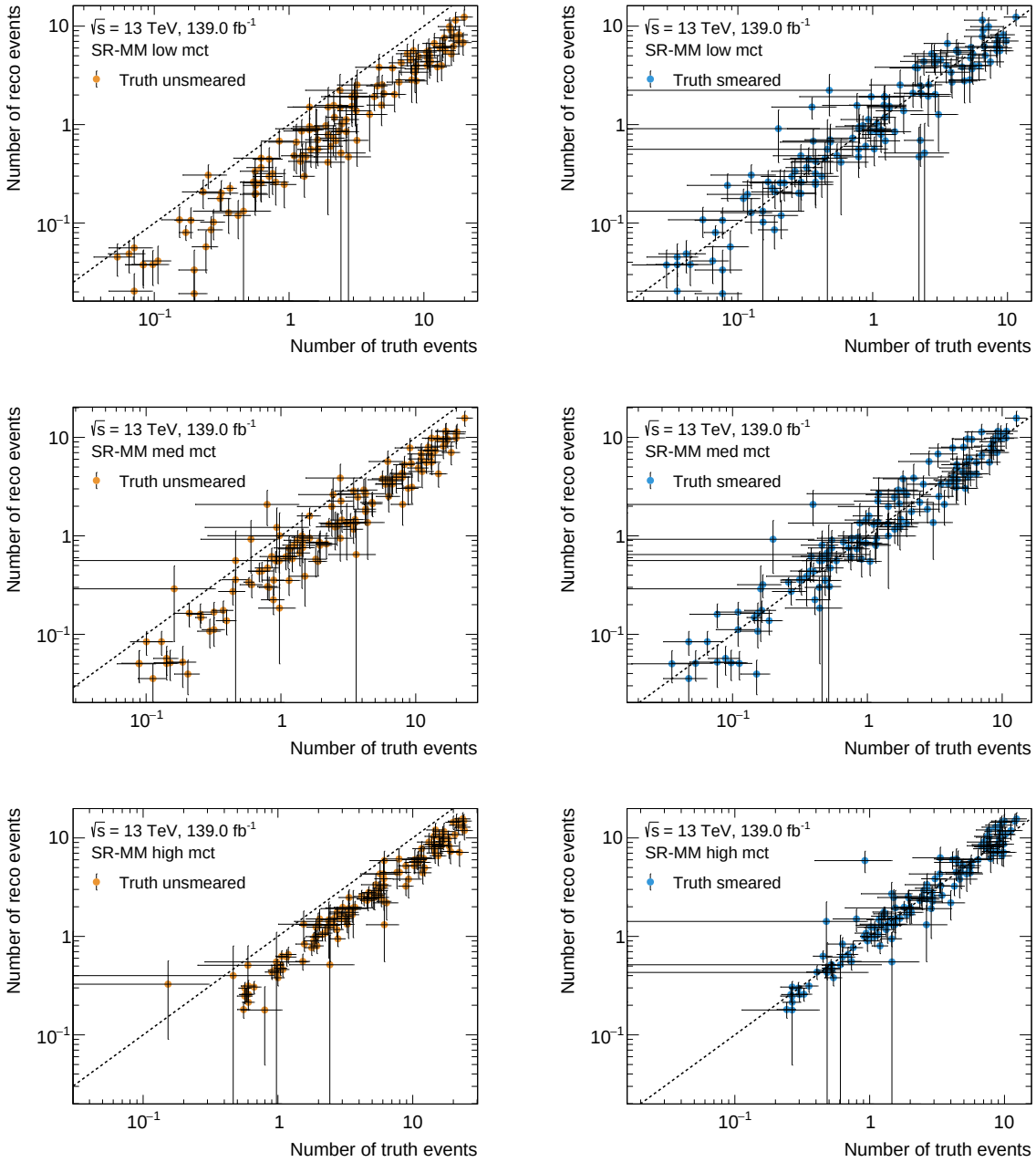

Figure C.2: Comparison of the event rates at truth- and reconstruction-level before (left) and after (right) truth smearing in SR-MM. From top to bottom, the low, medium and high m_{CT} bins are shown. Every single point in the scatter plots represents a single signal model considered in the original 1-lepton analysis. Uncertainties include only MC statistical uncertainties.

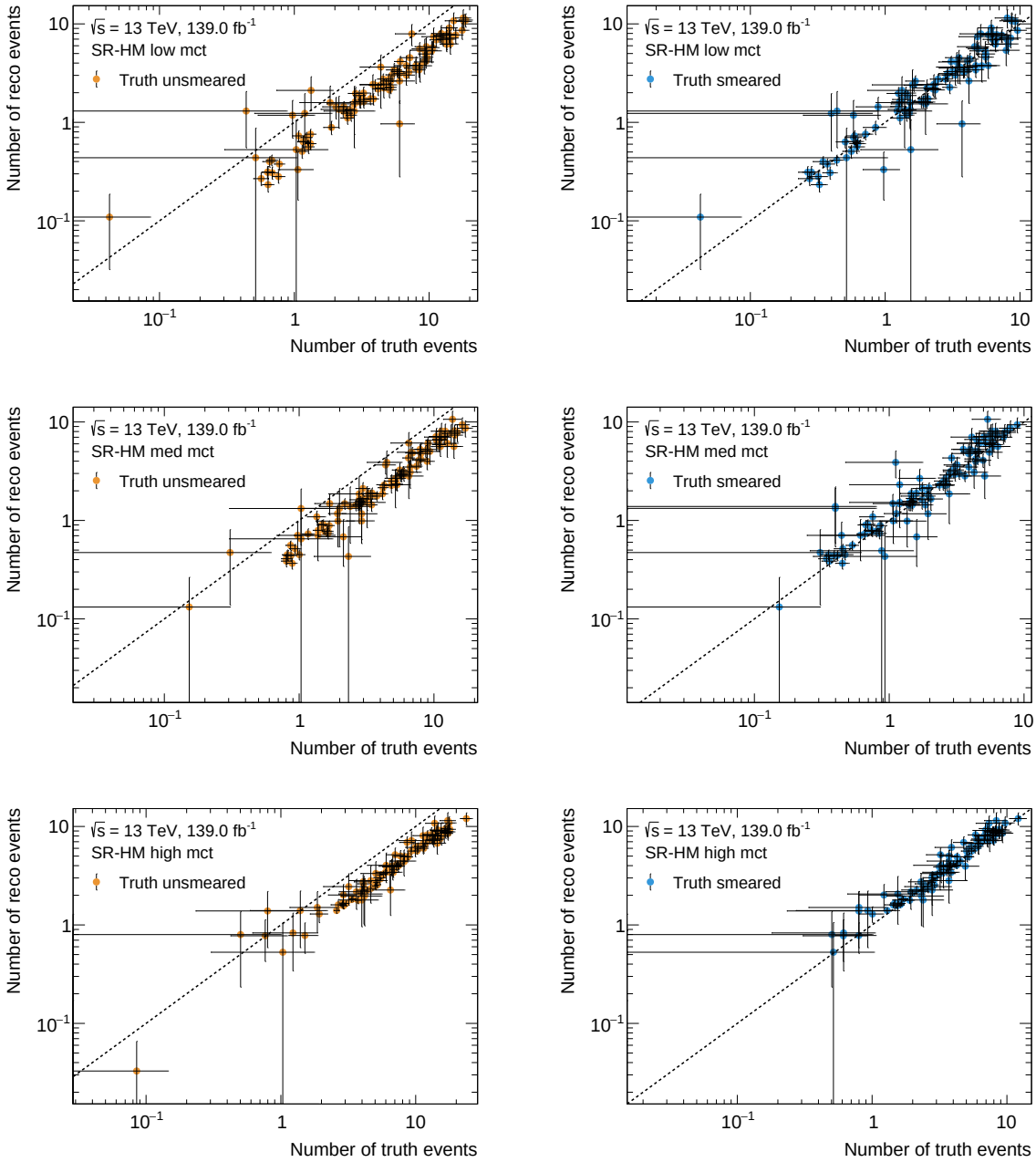

Figure C.3: Comparison of the event rates at truth- and reconstruction-level before (left) and after (right) truth smearing in SR-HM. From top to bottom, the low, medium and high m_{CT} bins are shown. Every single point in the scatter plots represents a single signal model considered in the original 1-lepton analysis. Uncertainties include only MC statistical uncertainties.

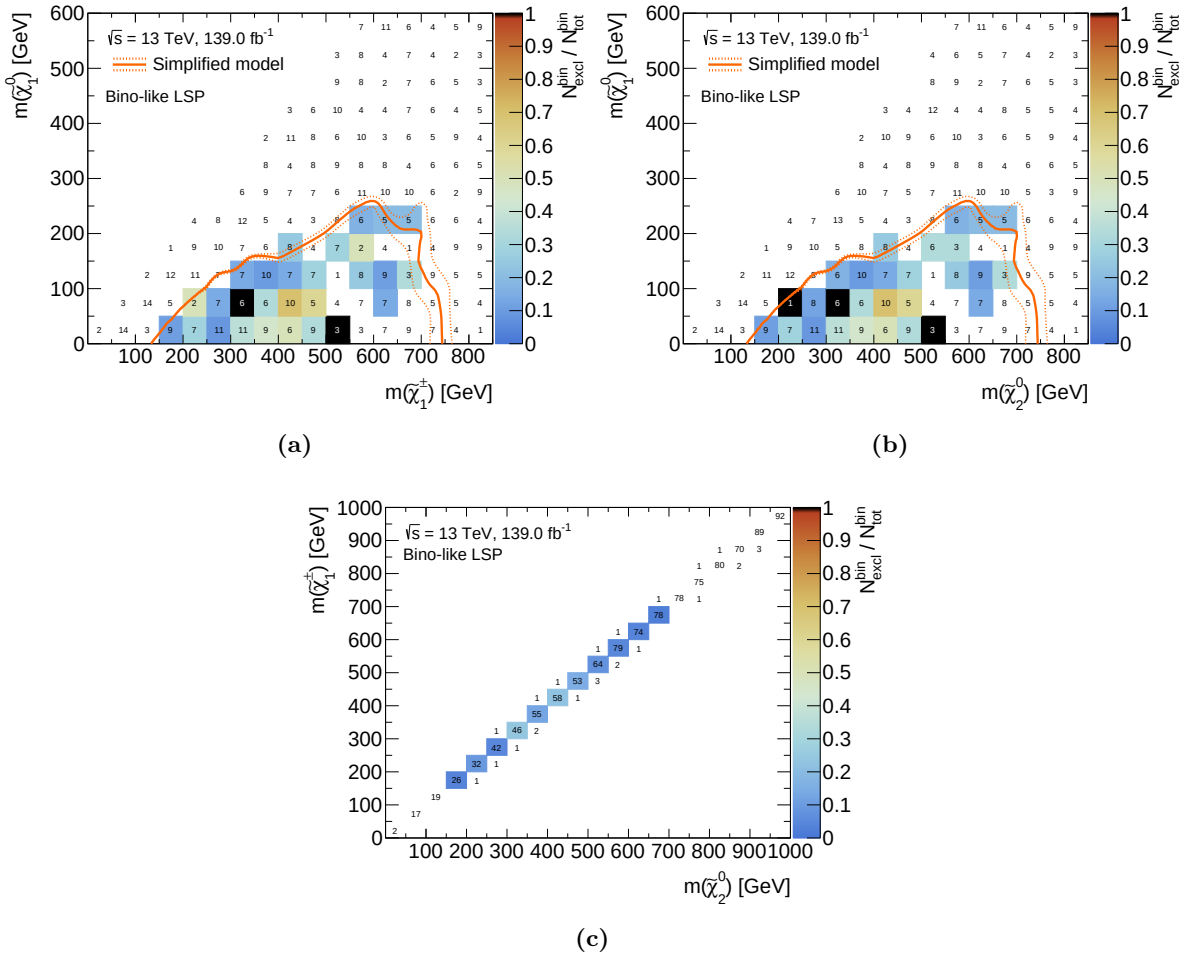

Figure C.4: Bin-by-bin fraction of excluded models as a function of the relevant sparticle masses. Only pMSSM models with a bino-like LSP are shown. The numbers in the bins correspond to the total number of models sampled falling into the respective bin. The number of models excluded by the 1-lepton analysis is encoded with a colour bar ranging from 0 to 1. Where all models in a given bin are excluded, the bin is coloured in black. Bins without a models excluded are left white. Models are evaluated using the simplified likelihood of the 1-lepton analysis. The simplified model contour is shown in orange.

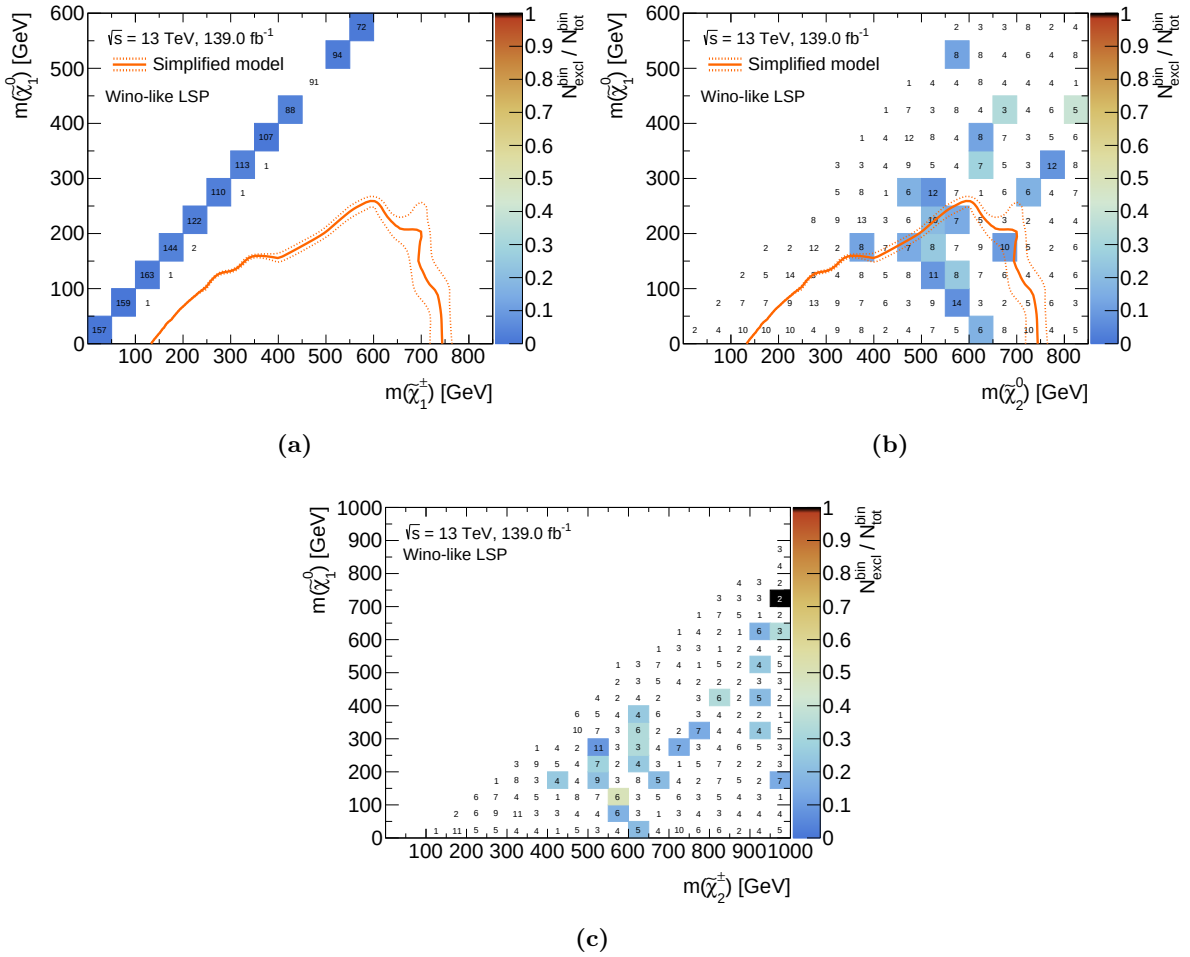

Figure C.5: Bin-by-bin fraction of excluded models as a function of the relevant sparticle masses. Only pMSSM models with a wino-like LSP are shown. The numbers in the bins correspond to the total number of models sampled falling into the respective bin. The number of models excluded by the 1-lepton analysis is encoded with a colour bar ranging from 0 to 1. Where all models in a given bin are excluded, the bin is coloured in black. Bins without a models excluded are left white. Models are evaluated using the simplified likelihood of the 1-lepton analysis. The simplified model contour is shown in orange.

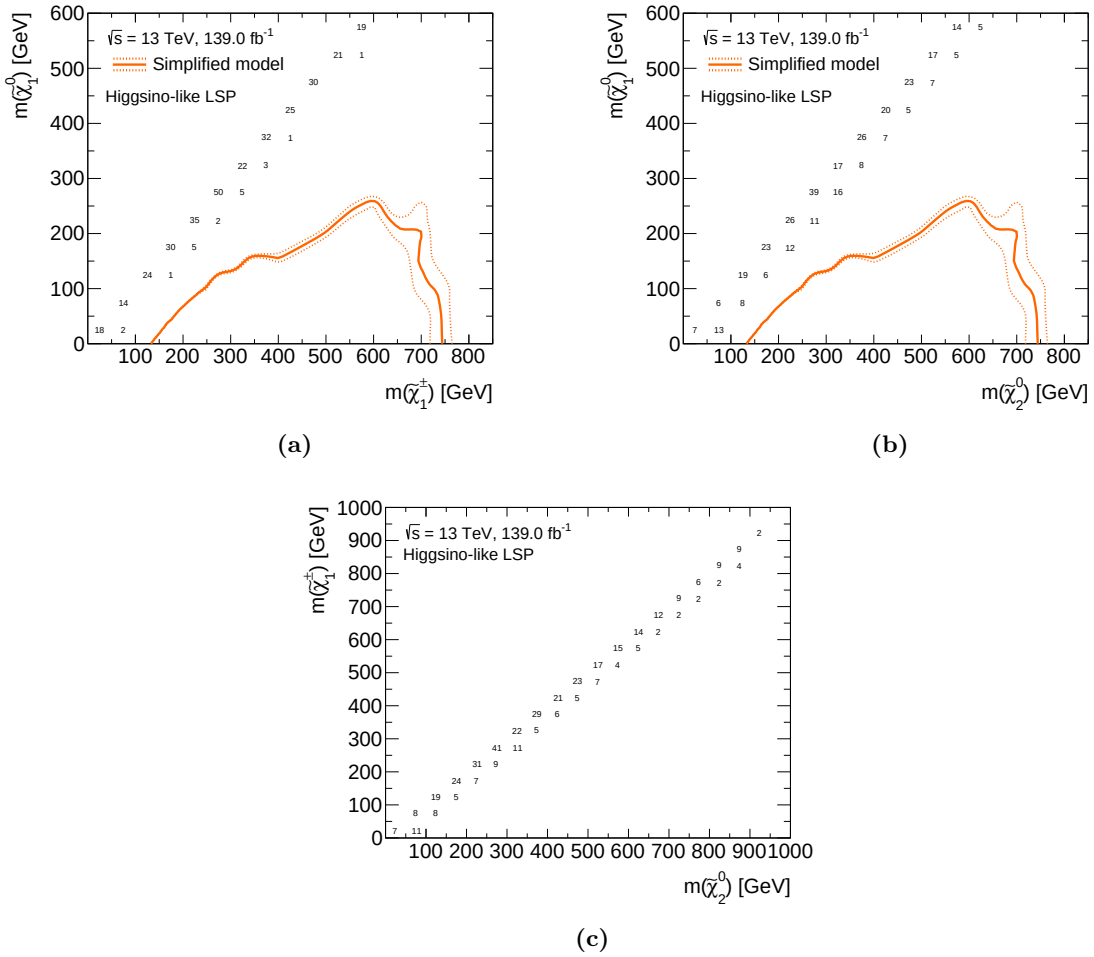

Figure C.6: Bin-by-bin fraction of excluded models as a function of the relevant sparticle masses. Only pMSSM models with a higgsino-like LSP are shown. The numbers in the bins correspond to the total number of models sampled falling into the respective bin. The number of models excluded by the 1-lepton analysis is encoded with a colour bar ranging from 0 to 1. Where all models in a given bin are excluded, the bin is coloured in black. Bins without a models excluded are left white. Models are evaluated using the simplified likelihood of the 1-lepton analysis. The simplified model contour is shown in orange.

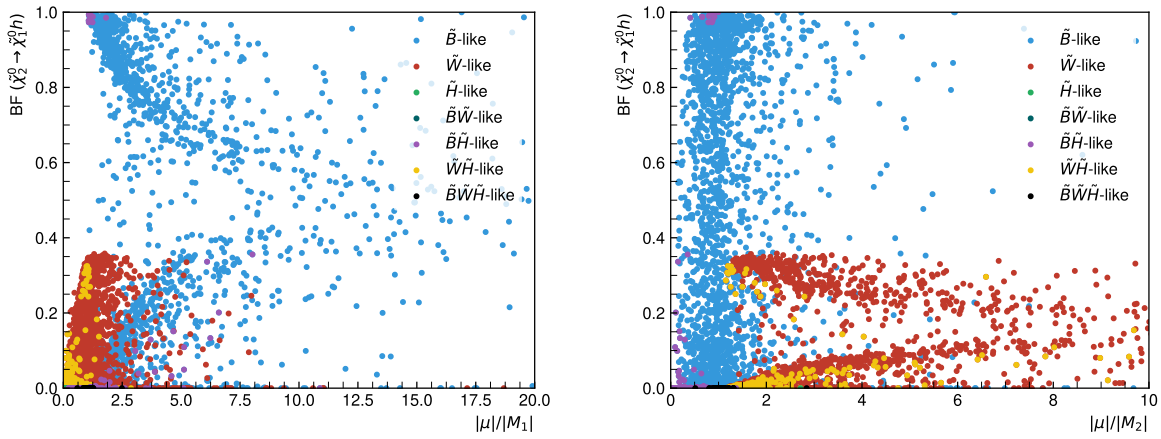

(a) (b)

Figure C.7

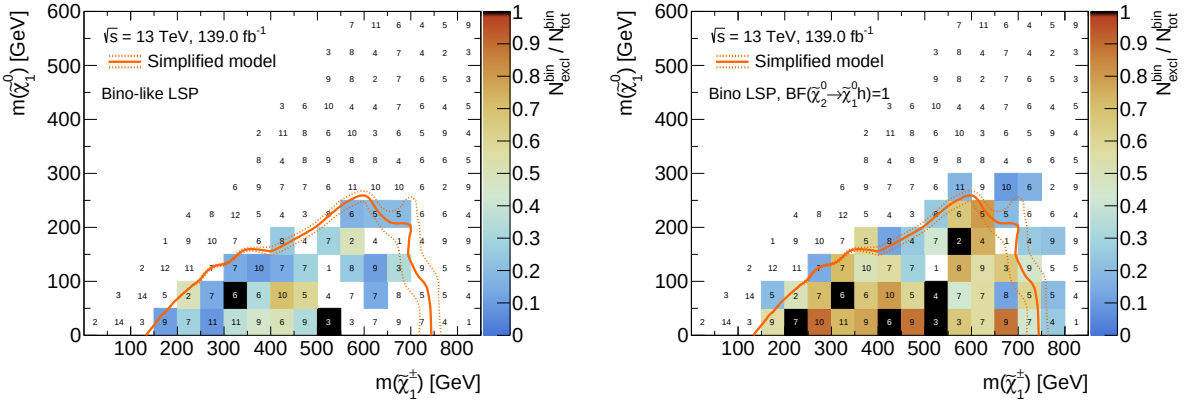

(a) (b)

Figure C.8

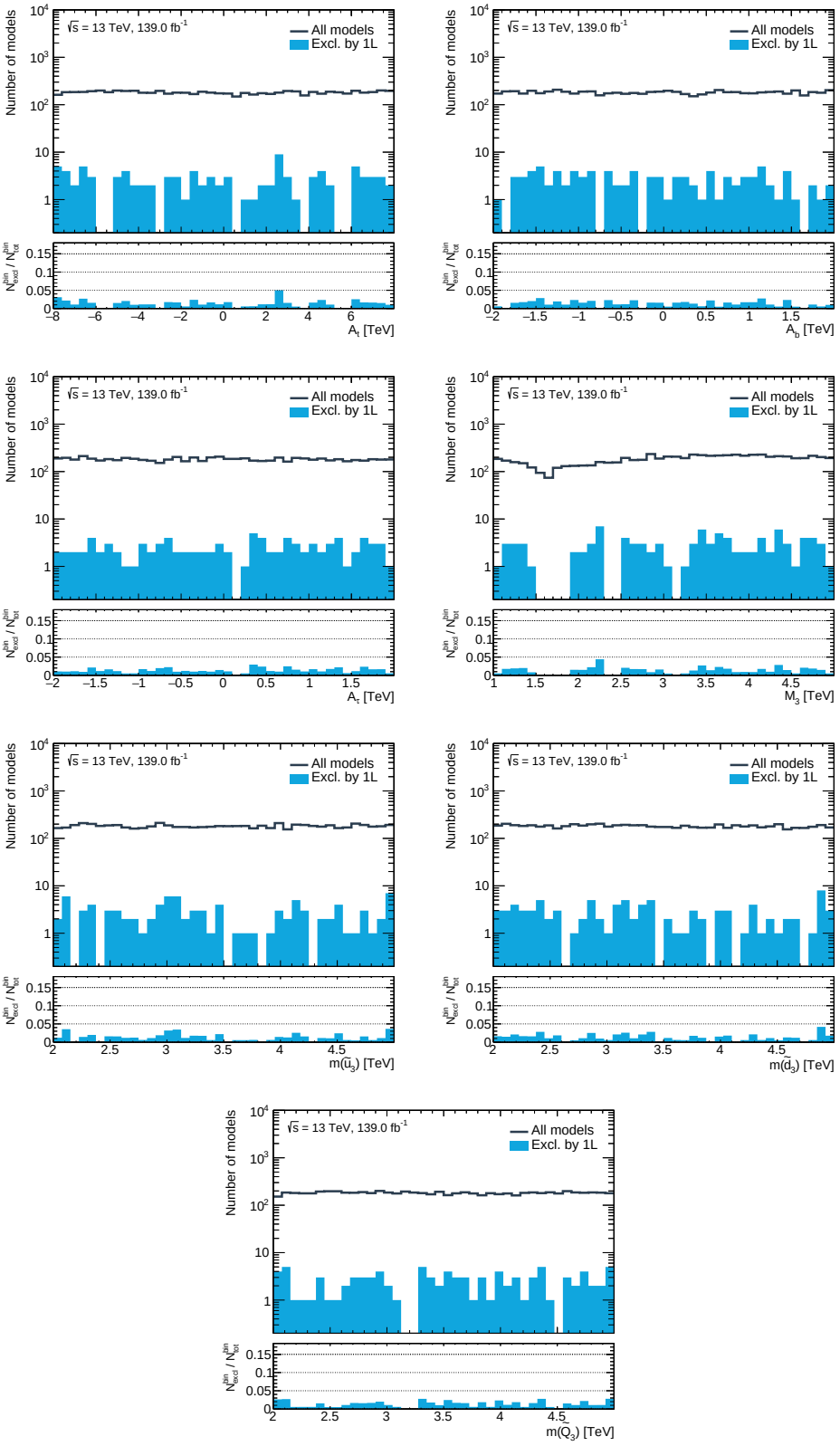
√s = 13 TeV, 139.0 fb-1
All models
Excl. by 1L
Number of models
$N^{bin}_{excl} / N^{bin}_{tot}$
A_t [TeV]
A_b [TeV]
A_τ [TeV]
M_3 [TeV]
$m(\tilde{u}_3)$ [TeV]
$m(\tilde{d}_3)$ [TeV]
$m(\tilde{Q}_3)$ [TeV]

Figure C.9

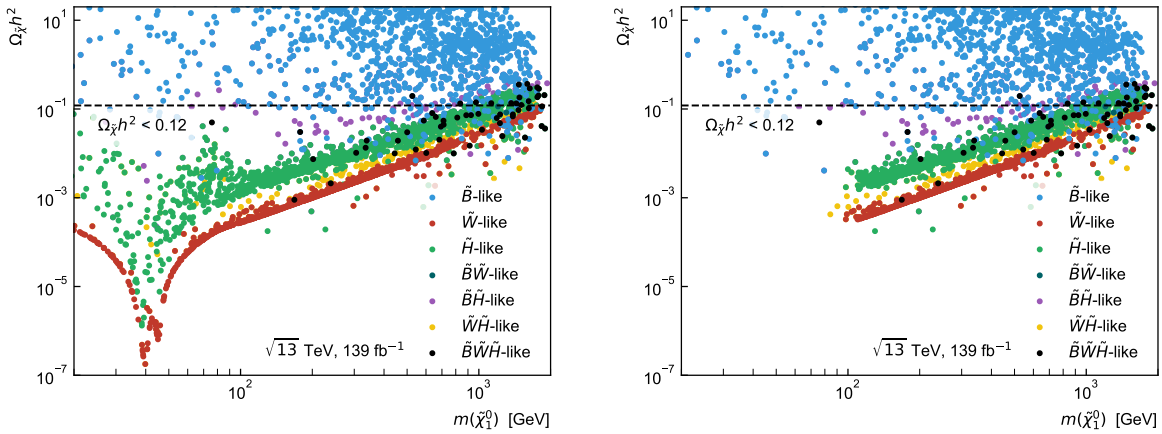

(a) **(b)**

Figure C.10

Abbreviations

BSM beyond the Standard Model. 147, 154

DM dark matter. 161, 163, 164

ID inner detector. 150

JER jet energy resolution. 150

LEP Large Electron Positron. 156, 163

LHC Large Hadron Collider. 154

LSP lightest supersymmetric particle. 156–158, 160, 161, 183–185

MC Monte Carlo. 149, 151–153, 180–182

ME matrix element. 156

MS muon spectrometer. 150

NLO next-to-leading order. 155

PDF parton distribution function. 156

pMSSM phenomenological Minimal Supersymmetric Standard Model. 147, 154–158, 160, 161, 163, 164, 183–185

PS parton shower. 156

SR signal region. 152

SUSY Supersymmetry. 147–149, 154–156, 163, 164

Bibliography

[1] I. C. Brock and T. Schorner-Sadenius, *Physics at the terascale*. Wiley, Weinheim, 2011. https://cds.cern.ch/record/1354959.

[2] M. E. Peskin and D. V. Schroeder, *An Introduction to quantum field theory*. Addison-Wesley, Reading, USA, 1995. http://www.slac.stanford.edu/~mpeskin/QFT.html.

[3] S. P. Martin, "A Supersymmetry primer," arXiv:hep-ph/9709356 [hep-ph]. [Adv. Ser. Direct. High Energy Phys.18,1(1998)].

[4] M. Bustamante, L. Cieri, and J. Ellis, "Beyond the Standard Model for Montaneros," in *5th CERN - Latin American School of High-Energy Physics*. 11, 2009. arXiv:0911.4409 [hep-ph].

[5] L. Brown, *The Birth of particle physics*. Cambridge University Press, Cambridge Cambridgeshire New York, 1986.

[6] P. J. Mohr, D. B. Newell, and B. N. Taylor, "CODATA Recommended Values of the Fundamental Physical Constants: 2014," *Rev. Mod. Phys.* **88** no. 3, (2016) 035009, arXiv:1507.07956 [physics.atom-ph].

[7] P. D. Group, "Review of Particle Physics," *Progress of Theoretical and Experimental Physics* **2020** no. 8, (08, 2020) , https://academic.oup.com/ptep/article-pdf/2020/8/083C01/34673722/ptaa104.pdf. https://doi.org/10.1093/ptep/ptaa104. 083C01.

[8] **Super-Kamiokande** Collaboration, Y. Fukuda *et al.*, "Evidence for oscillation of atmospheric neutrinos," *Phys. Rev. Lett.* **81** (1998) 1562–1567, arXiv:hep-ex/9807003 [hep-ex].

[9] Z. Maki, M. Nakagawa, and S. Sakata, "Remarks on the unified model of elementary particles," *Prog. Theor. Phys.* **28** (1962) 870–880. [,34(1962)].

[10] N. Cabibbo, "Unitary symmetry and leptonic decays," *Phys. Rev. Lett.* **10** (Jun, 1963) 531–533. https://link.aps.org/doi/10.1103/PhysRevLett.10.531.

[11] M. Kobayashi and T. Maskawa, "CP Violation in the Renormalizable Theory of Weak Interaction," *Prog. Theor. Phys.* **49** (1973) 652–657.

[12] E. Noether and M. A. Tavel, "Invariant variation problems," arXiv:physics/0503066.

[13] J. C. Ward, "An identity in quantum electrodynamics," *Phys. Rev.* **78** (Apr, 1950) 182–182. https://link.aps.org/doi/10.1103/PhysRev.78.182.

[14] Y. Takahashi, "On the generalized ward identity," *Il Nuovo Cimento (1955-1965)* **6** no. 2, (Aug, 1957) 371–375. https://doi.org/10.1007/BF02832514.

[15] G. 'tHooft, "Renormalization of massless yang-mills fields," *Nuclear Physics B* **33** no. 1, (1971) 173 – 199. http://www.sciencedirect.com/science/article/pii/0550321371903956.

[16] J. Taylor, "Ward identities and charge renormalization of the yang-mills field," *Nuclear Physics B* **33** no. 2, (1971) 436 – 444. http://www.sciencedirect.com/science/article/pii/0550321371902975.

[17] A. A. Slavnov, "Ward identities in gauge theories," *Theoretical and Mathematical Physics* **10** no. 2, (Feb, 1972) 99–104. https://doi.org/10.1007/BF01090719.

[18] C. N. Yang and R. L. Mills, "Conservation of isotopic spin and isotopic gauge invariance," *Phys. Rev.* **96** (Oct, 1954) 191–195. https://link.aps.org/doi/10.1103/PhysRev.96.191.

[19] K. G. Wilson, "Confinement of quarks," *Phys. Rev. D* **10** (Oct, 1974) 2445–2459. https://link.aps.org/doi/10.1103/PhysRevD.10.2445.

[20] T. DeGrand and C. DeTar, *Lattice Methods for Quantum Chromodynamics*. World Scientific, Singapore, 2006. https://cds.cern.ch/record/1055545.

[21] S. L. Glashow, "Partial-symmetries of weak interactions," *Nuclear Physics* **22** no. 4, (1961) 579 – 588. http://www.sciencedirect.com/science/article/pii/0029558261904692.

[22] S. Weinberg, "A model of leptons," *Phys. Rev. Lett.* **19** (Nov, 1967) 1264–1266. https://link.aps.org/doi/10.1103/PhysRevLett.19.1264.

[23] A. Salam and J. C. Ward, "Weak and electromagnetic interactions," *Il Nuovo Cimento (1955-1965)* **11** no. 4, (Feb, 1959) 568–577. https://doi.org/10.1007/BF02726525.

[24] C. S. Wu, E. Ambler, R. W. Hayward, D. D. Hoppes, and R. P. Hudson, "Experimental test of parity conservation in beta decay," *Phys. Rev.* **105** (Feb, 1957) 1413–1415. https://link.aps.org/doi/10.1103/PhysRev.105.1413.

[25] M. Gell-Mann, "The interpretation of the new particles as displaced charge multiplets," *Il Nuovo Cimento (1955-1965)* **4** no. 2, (Apr, 1956) 848–866. https://doi.org/10.1007/BF02748000.

[26] K. Nishijima, "Charge Independence Theory of V Particles*," *Progress of Theoretical Physics* **13** no. 3, (03, 1955) 285–304, https://academic.oup.com/ptp/article-pdf/13/3/285/5425869/13-3-285.pdf. https://doi.org/10.1143/PTP.13.285.

[27] T. Nakano and K. Nishijima, "Charge Independence for V-particles*," *Progress of Theoretical Physics* **10** no. 5, (11, 1953) 581–582, https://academic.oup.com/ptp/article-pdf/10/5/581/5364926/10-5-581.pdf. https://doi.org/10.1143/PTP.10.581.

[28] F. Englert and R. Brout, "Broken symmetry and the mass of gauge vector mesons," *Phys. Rev. Lett.* **13** (Aug, 1964) 321–323. https://link.aps.org/doi/10.1103/PhysRevLett.13.321.

[29] P. W. Higgs, "Broken symmetries and the masses of gauge bosons," *Phys. Rev. Lett.* **13** (Oct, 1964) 508–509. https://link.aps.org/doi/10.1103/PhysRevLett.13.508.

[30] P. W. Higgs, "Spontaneous symmetry breakdown without massless bosons," *Phys. Rev.* **145** (May, 1966) 1156–1163. https://link.aps.org/doi/10.1103/PhysRev.145.1156.

[31] Y. Nambu, "Quasiparticles and Gauge Invariance in the Theory of Superconductivity," *Phys. Rev.* **117** (1960) 648–663. [,132(1960)].

[32] J. Goldstone, "Field Theories with Superconductor Solutions," *Nuovo Cim.* **19** (1961) 154–164.

[33] V. Brdar, A. J. Helmboldt, S. Iwamoto, and K. Schmitz, "Type-I Seesaw as the Common Origin of Neutrino Mass, Baryon Asymmetry, and the Electroweak Scale," *Phys. Rev. D* **100** (2019) 075029, arXiv:1905.12634 [hep-ph].

[34] G. 't Hooft and M. Veltman, "Regularization and renormalization of gauge fields," *Nuclear Physics B* **44** no. 1, (1972) 189 – 213. http://www.sciencedirect.com/science/article/pii/0550321372902799.

[35] F. Zwicky, "Die Rotverschiebung von extragalaktischen Nebeln," *Helv. Phys. Acta* **6** (1933) 110–127. https://cds.cern.ch/record/437297.

[36] V. C. Rubin and W. K. Ford, Jr., "Rotation of the Andromeda Nebula from a Spectroscopic Survey of Emission Regions," *Astrophys. J.* **159** (1970) 379–403.

[37] G. Bertone, D. Hooper, and J. Silk, "Particle dark matter: Evidence, candidates and constraints," *Phys. Rept.* **405** (2005) 279–390, arXiv:hep-ph/0404175.

[38] D. Clowe, M. Bradac, A. H. Gonzalez, M. Markevitch, S. W. Randall, C. Jones, and D. Zaritsky, "A direct empirical proof of the existence of dark matter," *Astrophys. J.* **648** (2006) L109–L113, arXiv:astro-ph/0608407 [astro-ph].

[39] A. Taylor, S. Dye, T. J. Broadhurst, N. Benitez, and E. van Kampen, "Gravitational lens magnification and the mass of abell 1689," *Astrophys. J.* **501** (1998) 539, arXiv:astro-ph/9801158.

[40] C. Bennett *et al.*, "Four year COBE DMR cosmic microwave background observations: Maps and basic results," *Astrophys. J. Lett.* **464** (1996) L1–L4, arXiv:astro-ph/9601067.

[41] G. F. Smoot *et al.*, "Structure in the COBE Differential Microwave Radiometer First-Year Maps," *ApJS* **396** (September, 1992) L1.

[42] **WMAP** Collaboration, "Nine-year Wilkinson Microwave Anisotropy Probe (WMAP) Observations: Final Maps and Results," *ApJS* **208** no. 2, (October, 2013) 20, arXiv:1212.5225 [astro-ph.CO].

[43] **WMAP** Collaboration, "Nine-year Wilkinson Microwave Anisotropy Probe (WMAP) Observations: Cosmological Parameter Results," *ApJS* **208** no. 2, (October, 2013) 19, arXiv:1212.5226 [astro-ph.CO].

[44] **Planck** Collaboration, "Planck 2018 results. I. Overview and the cosmological legacy of Planck," *Astron. Astrophys.* **641** (2020) A1, arXiv:1807.06205 [astro-ph.CO].

[45] A. Liddle, *An introduction to modern cosmology; 3rd ed.* Wiley, Chichester, Mar, 2015. https://cds.cern.ch/record/1976476.

[46] **Planck** Collaboration, "Planck 2018 results. VI. Cosmological parameters," *Astron. Astrophys.* **641** (2020) A6, arXiv:1807.06209 [astro-ph.CO].

[47] H. Georgi and S. L. Glashow, "Unity of all elementary-particle forces," *Phys. Rev. Lett.* **32** (Feb, 1974) 438–441. https://link.aps.org/doi/10.1103/PhysRevLett.32.438.

[48] I. Aitchison, *Supersymmetry in Particle Physics. An Elementary Introduction*. Cambridge University Press, Cambridge, 2007.

[49] **Muon g-2** Collaboration, G. Bennett *et al.*, "Final Report of the Muon E821 Anomalous Magnetic Moment Measurement at BNL," *Phys. Rev. D* **73** (2006) 072003, arXiv:hep-ex/0602035.

[50] H. Baer and X. Tata, *Weak Scale Supersymmetry: From Superfields to Scattering Events*. Cambridge University Press, 2006.

[51] A. Czarnecki and W. J. Marciano, "The Muon anomalous magnetic moment: A Harbinger for 'new physics'," *Phys. Rev. D* **64** (2001) 013014, arXiv:hep-ph/0102122.

[52] J. L. Feng and K. T. Matchev, "Supersymmetry and the anomalous magnetic moment of the muon," *Phys. Rev. Lett.* **86** (2001) 3480–3483, arXiv:hep-ph/0102146.

[53] S. Coleman and J. Mandula, "All possible symmetries of the s matrix," *Phys. Rev.* **159** (Jul, 1967) 1251–1256. https://link.aps.org/doi/10.1103/PhysRev.159.1251.

[54] R. Haag, J. T. Lopuszanski, and M. Sohnius, "All Possible Generators of Supersymmetries of the s Matrix," *Nucl. Phys.* **B88** (1975) 257. [,257(1974)].

[55] J. Wess and B. Zumino, "Supergauge transformations in four dimensions," *Nuclear Physics B* **70** no. 1, (1974) 39 – 50. http://www.sciencedirect.com/science/article/pii/0550321374903551.

[56] H. Georgi and S. L. Glashow, "Gauge theories without anomalies," *Phys. Rev. D* **6** (Jul, 1972) 429–431. https://link.aps.org/doi/10.1103/PhysRevD.6.429.

[57] S. Dimopoulos and D. W. Sutter, "The Supersymmetric flavor problem," *Nucl. Phys. B* **452** (1995) 496–512, arXiv:hep-ph/9504415.

[58] **MEG** Collaboration, T. Mori, "Final Results of the MEG Experiment," *Nuovo Cim. C* **39** no. 4, (2017) 325, arXiv:1606.08168 [hep-ex].

[59] H. P. Nilles, "Supersymmetry, Supergravity and Particle Physics," *Phys. Rept.* **110** (1984) 1–162.

[60] A. Lahanas and D. Nanopoulos, "The road to no-scale supergravity," *Physics Reports* **145** no. 1, (1987) 1 – 139. http://www.sciencedirect.com/science/article/pii/0370157387900342.

[61] J. L. Feng, A. Rajaraman, and F. Takayama, "Superweakly interacting massive particles," *Phys. Rev. Lett.* **91** (2003) 011302, arXiv:hep-ph/0302215.

[62] **Super-Kamiokande** Collaboration, K. Abe *et al.*, "Search for proton decay via $p \to e^+\pi^0$ and $p \to \mu^+\pi^0$ in 0.31 megaton-years exposure of the Super-Kamiokande water Cherenkov detector," *Phys. Rev.* **D95** no. 1, (2017) 012004, arXiv:1610.03597 [hep-ex].

[63] J. R. Ellis, "Beyond the standard model for hill walkers," in *1998 European School of High-Energy Physics*, pp. 133–196. 8, 1998. arXiv:hep-ph/9812235.

[64] J. R. Ellis, J. Hagelin, D. V. Nanopoulos, K. A. Olive, and M. Srednicki, "Supersymmetric Relics from the Big Bang," *Nucl. Phys. B* **238** (1984) 453–476.

[65] D. O. Caldwell, R. M. Eisberg, D. M. Grumm, M. S. Witherell, B. Sadoulet, F. S. Goulding, and A. R. Smith, "Laboratory limits on galactic cold dark matter," *Phys. Rev. Lett.* **61** (Aug, 1988) 510–513. https://link.aps.org/doi/10.1103/PhysRevLett.61.510.

[66] M. Mori, M. M. Nojiri, K. S. Hirata, K. Kihara, Y. Oyama, A. Suzuki, K. Takahashi, M. Yamada, H. Takei, M. Koga, K. Miyano, H. Miyata, Y. Fukuda, T. Hayakawa, K. Inoue, T. Ishida, T. Kajita, Y. Koshio, M. Nakahata, K. Nakamura, A. Sakai, N. Sato, M. Shiozawa, J. Suzuki, Y. Suzuki, Y. Totsuka, M. Koshiba, K. Nishijima, T. Kajimura, T. Suda, A. T. Suzuki, T. Hara, Y. Nagashima, M. Takita, H. Yokoyama, A. Yoshimoto, K. Kaneyuki, Y. Takeuchi, T. Tanimori, S. Tasaka, and K. Nishikawa, "Search for neutralino dark matter heavier than the w boson at kamiokande," *Phys. Rev. D* **48** (Dec, 1993) 5505–5518. https://link.aps.org/doi/10.1103/PhysRevD.48.5505.

[67] **CDMS** Collaboration, D. S. Akerib *et al.*, "Exclusion limits on the WIMP-nucleon cross section from the first run of the Cryogenic Dark Matter Search in the Soudan Underground Laboratory," *Phys. Rev. D* **72** (2005) 052009, arXiv:astro-ph/0507190.

[68] A. Djouadi, J.-L. Kneur, and G. Moultaka, "SuSpect: A Fortran code for the supersymmetric and Higgs particle spectrum in the MSSM," *Comput. Phys. Commun.* **176** (2007) 426–455, arXiv:hep-ph/0211331.

[69] C. F. Berger, J. S. Gainer, J. L. Hewett, and T. G. Rizzo, "Supersymmetry without prejudice," *Journal of High Energy Physics* **2009** no. 02, (Feb, 2009) 023–023. http://dx.doi.org/10.1088/1126-6708/2009/02/023.

[70] J. Alwall, P. Schuster, and N. Toro, "Simplified Models for a First Characterization of New Physics at the LHC," *Phys. Rev.* **D79** (2009) 075020, arXiv:0810.3921 [hep-ph].

[71] **LHC New Physics Working Group** Collaboration, D. Alves, "Simplified Models for LHC New Physics Searches," *J. Phys.* **G39** (2012) 105005, arXiv:1105.2838 [hep-ph].

[72] D. S. Alves, E. Izaguirre, and J. G. Wacker, "Where the Sidewalk Ends: Jets and Missing Energy Search Strategies for the 7 TeV LHC," *JHEP* **10** (2011) 012, arXiv:1102.5338 [hep-ph].

[73] F. Ambrogi, S. Kraml, S. Kulkarni, U. Laa, A. Lessa, and W. Waltenberger, "On the coverage of the pMSSM by simplified model results," *Eur. Phys. J. C* **78** no. 3, (2018) 215, arXiv:1707.09036 [hep-ph].

[74] O. Buchmueller and J. Marrouche, "Universal mass limits on gluino and third-generation squarks in the context of Natural-like SUSY spectra," *Int. J. Mod. Phys. A* **29** no. 06, (2014) 1450032, arXiv:1304.2185 [hep-ph].

[75] **ATLAS** Collaboration, M. Aaboud *et al.*, "Dark matter interpretations of ATLAS searches for the electroweak production of supersymmetric particles in $\sqrt{s} = 8$ TeV proton-proton collisions," *JHEP* **09** (2016) 175, arXiv:1608.00872 [hep-ex].

[76] **ATLAS** Collaboration, "Summary of the ATLAS experiment's sensitivity to supersymmetry after LHC Run 1 — interpreted in the phenomenological MSSM," *JHEP* **10** (2015) 134, arXiv:1508.06608 [hep-ex].

[77] **ATLAS** Collaboration, "Mass reach of the atlas searches for supersymmetry." https://atlas.web.cern.ch/Atlas/GROUPS/PHYSICS/PUBNOTES/ATL-PHYS-PUB-2020-020/fig_23.png, 2020.

[78] **CMS** Collaboration, "Summary plot moriond 2017." https://twiki.cern.ch/twiki/pub/CMSPublic/SUSYSummary2017/Moriond2017_BarPlot.pdf, 2017.

[79] L. S. W. Group, "Notes lepsusywg/02-04.1 and lepsusywg/01-03.1." http://lepsusy.web.cern.ch/lepsusy/, 2004. Accessed: 2021-02-11.

[80] **ATLAS** Collaboration, G. Aad *et al.*, "Observation of a new particle in the search for the Standard Model Higgs boson with the ATLAS detector at the LHC," *Phys. Lett. B* **716** (2012) 1–29, arXiv:1207.7214 [hep-ex].

[81] **CMS** Collaboration, S. Chatrchyan *et al.*, "Observation of a New Boson at a Mass of 125 GeV with the CMS Experiment at the LHC," *Phys. Lett. B* **716** (2012) 30–61, arXiv:1207.7235 [hep-ex].

[82] CERN, "About cern." https://home.cern/about. Accessed: 2021-01-21.

[83] CERN, "CERN Annual report 2019," tech. rep., CERN, Geneva, 2020. https://cds.cern.ch/record/2723123.

[84] O. S. Bruning, P. Collier, P. Lebrun, S. Myers, R. Ostojic, J. Poole, and P. Proudlock, *LHC Design Report*. CERN Yellow Reports: Monographs. CERN, Geneva, 2004. https://cds.cern.ch/record/782076.

[85] M. Blewett and N. Vogt-Nilsen, "Proceedings of the 8th international conference on high-energy accelerators, cern 1971. conference held at geneva, 20–24 september 1971.," tech. rep., 1971, 1971.

[86] L. R. Evans and P. Bryant, "LHC Machine," *JINST* **3** (2008) S08001. 164 p. http://cds.cern.ch/record/1129806. This report is an abridged version of the LHC Design Report (CERN-2004-003).

[87] R. Scrivens, M. Kronberger, D. Küchler, J. Lettry, C. Mastrostefano, O. Midttun, M. O'Neil, H. Pereira, and C. Schmitzer, "Overview of the status and developments on primary ion sources at CERN*,". https://cds.cern.ch/record/1382102.

[88] M. Vretenar, J. Vollaire, R. Scrivens, C. Rossi, F. Roncarolo, S. Ramberger, U. Raich, B. Puccio, D. Nisbet, R. Mompo, S. Mathot, C. Martin, L. A. Lopez-Hernandez, A. Lombardi, J. Lettry, J. B. Lallement, I. Kozsar, J. Hansen, F. Gerigk, A. Funken, J. F. Fuchs, N. Dos Santos, M. Calviani, M. Buzio, O. Brunner, Y. Body, P. Baudrenghien, J. Bauche, and T. Zickler, *Linac4 design report*, vol. 6 of *CERN Yellow Reports: Monographs*. CERN, Geneva, 2020. https://cds.cern.ch/record/2736208.

[89] E. Mobs, "The CERN accelerator complex - 2019. Complexe des accélérateurs du CERN - 2019,". https://cds.cern.ch/record/2684277. General Photo.

[90] **ATLAS** Collaboration, "The ATLAS Experiment at the CERN Large Hadron Collider," *JINST* **3** (2008) S08003.

[91] **CMS** Collaboration, S. Chatrchyan *et al.*, "The CMS Experiment at the CERN LHC," *JINST* **3** (2008) S08004.

[92] **ALICE** Collaboration, K. Aamodt *et al.*, "The ALICE experiment at the CERN LHC," *JINST* **3** (2008) S08002.

[93] **LHCb** Collaboration, J. Alves, A.Augusto *et al.*, "The LHCb Detector at the LHC," *JINST* **3** (2008) S08005.

[94] **TOTEM** Collaboration, G. Anelli *et al.*, "The TOTEM experiment at the CERN Large Hadron Collider," *JINST* **3** (2008) S08007.

[95] **LHCf** Collaboration, O. Adriani *et al.*, "Technical design report of the LHCf experiment: Measurement of photons and neutral pions in the very forward region of LHC,".

[96] **MoEDAL** Collaboration, J. Pinfold *et al.*, "Technical Design Report of the MoEDAL Experiment,".

[97] **ATLAS** Collaboration, "ATLAS Public Results - Luminosity Public Results Run 2,". https://twiki.cern.ch/twiki/bin/view/AtlasPublic/LuminosityPublicResultsRun2. Accessed: 2021-01-17.

[98] **ATLAS** Collaboration, Z. Marshall, "Simulation of Pile-up in the ATLAS Experiment," *J. Phys. Conf. Ser.* **513** (2014) 022024.

[99] "First beam in the LHC - accelerating science,". https://home.cern/news/news/accelerators/record-luminosity-well-done-lhc. Accessed: 2021-01-10.

[100] **ATLAS Collaboration** Collaboration, "Luminosity determination in pp collisions at $\sqrt{s} = 13$ TeV using the ATLAS detector at the LHC," Tech. Rep. ATLAS-CONF-2019-021, CERN, Geneva, Jun, 2019. https://cds.cern.ch/record/2677054.

[101] **ATLAS** Collaboration, M. Aaboud *et al.*, "Luminosity determination in pp collisions at $\sqrt{s} = 8$ TeV using the ATLAS detector at the LHC," *Eur. Phys. J. C* **76** no. 12, (2016) 653, arXiv:1608.03953 [hep-ex].

[102] G. Avoni, M. Bruschi, G. Cabras, D. Caforio, N. Dehghanian, A. Floderus, B. Giacobbe, F. Giannuzzi, F. Giorgi, P. Grafström, V. Hedberg, F. L. Manghi, S. Meneghini, J. Pinfold, E. Richards, C. Sbarra, N. S. Cesari, A. Sbrizzi, R. Soluk, G. Ucchielli, S. Valentinetti, O. Viazlo, M. Villa, C. Vittori, R. Vuillermet, and A. Zoccoli, "The new LUCID-2 detector for luminosity measurement and monitoring in ATLAS," *Journal of Instrumentation* **13** no. 07, (Jul, 2018) P07017–P07017. https://doi.org/10.1088/1748-0221/13/07/p07017.

[103] S. van der Meer, "Calibration of the effective beam height in the ISR," Tech. Rep. CERN-ISR-PO-68-31. ISR-PO-68-31, CERN, Geneva, 1968. https://cds.cern.ch/record/296752.

[104] P. Grafström and W. Kozanecki, "Luminosity determination at proton colliders," *Progress in Particle and Nuclear Physics* **81** (2015) 97 – 148. http://www.sciencedirect.com/science/article/pii/S0146641014000878.

[105] "New schedule for CERN's accelerators and experiments,". https://home.cern/news/press-release/cern/first-beam-lhc-accelerating-science. Accessed: 2021-01-10.

[106] **ATLAS** Collaboration, G. Aad *et al.*, "Luminosity Determination in *pp* Collisions at $\sqrt{s} = 7$ TeV Using the ATLAS Detector at the LHC," *Eur. Phys. J. C* **71** (2011) 1630, arXiv:1101.2185 [hep-ex].

[107] **ATLAS Collaboration** Collaboration, G. Aad *et al.*, "Improved luminosity determination in pp collisions at $\sqrt{s} = 7$ TeV using the ATLAS detector at the LHC. Improved luminosity determination in pp collisions at sqrt(s) = 7 TeV using the ATLAS detector at the LHC," *Eur. Phys. J. C* **73** no. CERN-PH-EP-2013-026. CERN-PH-EP-2013-026, (Feb, 2013) 2518. 27 p. https://cds.cern.ch/record/1517411. Comments: 26 pages plus author list (39 pages total), 17 figures, 9 tables, submitted to EPJC, All figures are available at <a href=.

[108] "Record luminosity: well done LHC,". https://home.cern/news/news/accelerators/new-schedule-cerns-accelerators-and-experiments. Accessed: 2021-01-10.

[109] A. G., B. A. I., B. O., F. P., L. M., R. L., and T. L., *High-Luminosity Large Hadron Collider (HL-LHC): Technical Design Report V. 0.1*. CERN Yellow Reports: Monographs. CERN, Geneva, 2017. https://cds.cern.ch/record/2284929.

[110] J. Pequenao, "Computer generated image of the whole ATLAS detector." Mar, 2008.

[111] **ATLAS** Collaboration, "ATLAS: Detector and physics performance technical design report. Volume 1,".

[112] J. Pequenao, "Computer generated image of the ATLAS inner detector." Mar, 2008.

[113] **ATLAS Collaboration** Collaboration, K. Potamianos, "The upgraded Pixel detector and the commissioning of the Inner Detector tracking of the ATLAS experiment for Run-2 at the Large Hadron Collider," Tech. Rep. ATL-PHYS-PROC-2016-104, CERN, Geneva, Aug, 2016. https://cds.cern.ch/record/2209070. 15 pages, EPS-HEP 2015 Proceedings.

[114] **ATLAS IBL** Collaboration, B. Abbott *et al.*, "Production and Integration of the ATLAS Insertable B-Layer," *JINST* **13** no. 05, (2018) T05008, arXiv:1803.00844 [physics.ins-det].

[115] **ATLAS** Collaboration, "ATLAS Insertable B-Layer Technical Design Report," Tech. Rep. CERN-LHCC-2010-013. ATLAS-TDR-19, Sep, 2010. http://cds.cern.ch/record/1291633.

[116] **ATLAS** Collaboration, G. Aad *et al.*, "ATLAS b-jet identification performance and efficiency measurement with $t\bar{t}$ events in pp collisions at $\sqrt{s} = 13$ TeV," *Eur. Phys. J. C* **79** no. 11, (2019) 970, arXiv:1907.05120 [hep-ex].

[117] ATLAS Collaboration, "Particle Identification Performance of the ATLAS Transition Radiation Tracker." ATLAS-CONF-2011-128, 2011. https://cds.cern.ch/record/1383793.

[118] J. Pequenao, "Computer Generated image of the ATLAS calorimeter." Mar, 2008.

[119] J. Pequenao, "Computer generated image of the ATLAS Muons subsystem." Mar, 2008.

[120] S. Lee, M. Livan, and R. Wigmans, "Dual-Readout Calorimetry," *Rev. Mod. Phys.* **90** no. arXiv:1712.05494. 2, (Dec, 2017) 025002. 40 p. https://cds.cern.ch/record/2637852. 44 pages, 53 figures, accepted for publication in Review of Modern Physics.

[121] M. Leite, "Performance of the ATLAS Zero Degree Calorimeter," Tech. Rep. ATL-FWD-PROC-2013-001, CERN, Geneva, Nov, 2013. https://cds.cern.ch/record/1628749.

[122] S. Abdel Khalek *et al.*, "The ALFA Roman Pot Detectors of ATLAS," *JINST* **11** no. 11, (2016) P11013, arXiv:1609.00249 [physics.ins-det].

[123] U. Amaldi, G. Cocconi, A. Diddens, R. Dobinson, J. Dorenbosch, W. Duinker, D. Gustavson, J. Meyer, K. Potter, A. Wetherell, A. Baroncelli, and C. Bosio, "The real part of the forward proton proton scattering amplitude measured at the cern intersecting storage rings," *Physics Letters B* **66** no. 4, (1977) 390 – 394. http://www.sciencedirect.com/science/article/pii/0370269377900223.

[124] L. Adamczyk, E. Banaś, A. Brandt, M. Bruschi, S. Grinstein, J. Lange, M. Rijssenbeek, P. Sicho, R. Staszewski, T. Sykora, M. Trzebiński, J. Chwastowski, and K. Korcyl, "Technical Design Report for the ATLAS Forward Proton Detector," Tech. Rep. CERN-LHCC-2015-009. ATLAS-TDR-024, May, 2015. https://cds.cern.ch/record/2017378.

[125] **ATLAS** Collaboration, A. R. Martínez, "The Run-2 ATLAS Trigger System," *J. Phys. Conf. Ser.* **762** no. 1, (2016) 012003.

[126] **ATLAS Collaboration** Collaboration, *ATLAS level-1 trigger: Technical Design Report*. Technical Design Report ATLAS. CERN, Geneva, 1998. https://cds.cern.ch/record/381429.

[127] **ATLAS** Collaboration, G. Aad *et al.*, "Operation of the ATLAS trigger system in Run 2," *JINST* **15** no. 10, (2020) P10004, arXiv:2007.12539 [physics.ins-det].

[128] **ATLAS Collaboration** Collaboration, P. Jenni, M. Nessi, M. Nordberg, and K. Smith, *ATLAS high-level trigger, data-acquisition and controls: Technical Design Report*. Technical Design Report ATLAS. CERN, Geneva, 2003. https://cds.cern.ch/record/616089.

[129] **ATLAS** Collaboration, G. Aad *et al.*, "The ATLAS Simulation Infrastructure," *Eur. Phys. J. C* **70** (2010) 823–874, arXiv:1005.4568 [physics.ins-det].

[130] T. Gleisberg, S. Hoeche, F. Krauss, M. Schonherr, S. Schumann, F. Siegert, and J. Winter, "Event generation with SHERPA 1.1," *JHEP* **02** (2009) 007, arXiv:0811.4622 [hep-ph].

[131] A. Buckley *et al.*, "General-purpose event generators for LHC physics," *Phys. Rept.* **504** (2011) 145–233, arXiv:1101.2599 [hep-ph].

[132] V. N. Gribov and L. N. Lipatov, "Deep inelastic e p scattering in perturbation theory," *Sov. J. Nucl. Phys.* **15** (1972) 438–450.

[133] J. Blumlein, T. Doyle, F. Hautmann, M. Klein, and A. Vogt, "Structure functions in deep inelastic scattering at HERA," in *Workshop on Future Physics at HERA (To be followed by meetings 7-9 Feb and 30-31 May 1996 at DESY)*. 9, 1996. arXiv:hep-ph/9609425.

[134] A. Buckley, J. Ferrando, S. Lloyd, K. Nordström, B. Page, M. Rüfenacht, M. Schönherr, and G. Watt, "LHAPDF6: parton density access in the LHC precision era," *Eur. Phys. J. C* **75** (2015) 132, arXiv:1412.7420 [hep-ph].

[135] M. Bengtsson and T. Sjostrand, "Coherent Parton Showers Versus Matrix Elements: Implications of PETRA - PEP Data," *Phys. Lett. B* **185** (1987) 435.

[136] S. Catani, F. Krauss, R. Kuhn, and B. R. Webber, "QCD matrix elements + parton showers," *JHEP* **11** (2001) 063, arXiv:hep-ph/0109231.

[137] L. Lonnblad, "Correcting the color dipole cascade model with fixed order matrix elements," *JHEP* **05** (2002) 046, arXiv:hep-ph/0112284.

[138] B. Andersson, G. Gustafson, G. Ingelman, and T. Sjostrand, "Parton Fragmentation and String Dynamics," *Phys. Rept.* **97** (1983) 31–145.

[139] B. Andersson, *The Lund Model*. Cambridge Monographs on Particle Physics, Nuclear Physics and Cosmology. Cambridge University Press, 1998.

[140] D. Amati and G. Veneziano, "Preconfinement as a Property of Perturbative QCD," *Phys. Lett. B* **83** (1979) 87–92.

[141] D. Yennie, S. Frautschi, and H. Suura, "The infrared divergence phenomena and high-energy processes," *Annals of Physics* **13** no. 3, (1961) 379–452. https://www.sciencedirect.com/science/article/pii/0003491661901518.

[142] M. Dobbs and J. B. Hansen, "The HepMC C++ Monte Carlo event record for High Energy Physics," *Comput. Phys. Commun.* **134** (2001) 41–46.

[143] **GEANT4** Collaboration, S. Agostinelli *et al.*, "GEANT4: A Simulation toolkit," *Nucl. Instrum. Meth.* **A506** (2003) 250–303.

[144] **ATLAS Collaboration** Collaboration, "The new Fast Calorimeter Simulation in ATLAS," Tech. Rep. ATL-SOFT-PUB-2018-002, CERN, Geneva, Jul, 2018. https://cds.cern.ch/record/2630434.

[145] K. Cranmer, "Practical Statistics for the LHC," in *2011 European School of High-Energy Physics*, pp. 267–308. 2014. arXiv:1503.07622 [physics.data-an].

[146] G. Cowan, K. Cranmer, E. Gross, and O. Vitells, "Asymptotic formulae for likelihood-based tests of new physics," *Eur. Phys. J.* **C71** (2011) 1554, arXiv:1007.1727 [physics.data-an]. [Erratum: Eur. Phys. J.C73,2501(2013)].

[147] ATLAS Collaboration, "Reproduction searches for new physics with the ATLAS experiment through publication of full statistical likelihoods." ATL-PHYS-PUB-2019-029, 2019. https://cds.cern.ch/record/2684863.

[148] **ROOT Collaboration** Collaboration, K. Cranmer, G. Lewis, L. Moneta, A. Shibata, and W. Verkerke, "HistFactory: A tool for creating statistical models for use with RooFit and RooStats," Tech. Rep. CERN-OPEN-2012-016, New York U., New York, Jan, 2012. https://cds.cern.ch/record/1456844.

[149] W. Verkerke and D. P. Kirkby, "The RooFit toolkit for data modeling," *eConf* **C0303241** (2003) MOLT007, arXiv:physics/0306116 [physics]. [,186(2003)].

[150] L. Moneta, K. Belasco, K. S. Cranmer, S. Kreiss, A. Lazzaro, D. Piparo, G. Schott, W. Verkerke, and M. Wolf, "The RooStats Project," *PoS* **ACAT2010** (2010) 057, arXiv:1009.1003 [physics.data-an].

[151] F. James and M. Roos, "MINUIT: a system for function minimization and analysis of the parameter errors and corrections," *Comput. Phys. Commun.* **10** no. CERN-DD-75-20, (Jul, 1975) 343–367. 38 p. https://cds.cern.ch/record/310399.

[152] R. Brun and F. Rademakers, "ROOT: An object oriented data analysis framework," *Nucl. Instrum. Meth.* **A389** (1997) 81–86.

[153] I. Antcheva *et al.*, "Root — a c++ framework for petabyte data storage, statistical analysis and visualization," *Computer Physics Communications* **182** no. 6, (2011) 1384 – 1385. http://www.sciencedirect.com/science/article/pii/S0010465511000701.

[154] M. Baak, G. J. Besjes, D. Côte, A. Koutsman, J. Lorenz, and D. Short, "HistFitter software framework for statistical data analysis," *Eur. Phys. J.* **C75** (2015) 153, `arXiv:1410.1280 [hep-ex]`.

[155] L. Heinrich, M. Feickert, G. Stark, and K. Cranmer, "pyhf: pure-python implementation of histfactory statistical models," *Journal of Open Source Software* **6** no. 58, (2021) 2823. https://doi.org/10.21105/joss.02823.

[156] L. Heinrich, M. Feickert, and G. Stark, "pyhf: v0.6.0." https://github.com/scikit-hep/pyhf.

[157] C. R. Harris, K. J. Millman, S. J. van der Walt, R. Gommers, P. Virtanen, D. Cournapeau, E. Wieser, J. Taylor, S. Berg, N. J. Smith, R. Kern, M. Picus, S. Hoyer, M. H. van Kerkwijk, M. Brett, A. Haldane, J. F. del R'ıo, M. Wiebe, P. Peterson, P. G'erard-Marchant, K. Sheppard, T. Reddy, W. Weckesser, H. Abbasi, C. Gohlke, and T. E. Oliphant, "Array programming with NumPy," *Nature* **585** no. 7825, (Sept., 2020) 357–362. https://doi.org/10.1038/s41586-020-2649-2.

[158] A. Paszke, S. Gross, F. Massa, A. Lerer, J. Bradbury, G. Chanan, T. Killeen, Z. Lin, N. Gimelshein, L. Antiga, A. Desmaison, A. Kopf, E. Yang, Z. DeVito, M. Raison, A. Tejani, S. Chilamkurthy, B. Steiner, L. Fang, J. Bai, and S. Chintala, "Pytorch: An imperative style, high-performance deep learning library," in *Advances in Neural Information Processing Systems 32*, H. Wallach, H. Larochelle, A. Beygelzimer, F. d'Alché-Buc, E. Fox, and R. Garnett, eds., pp. 8024–8035. Curran Associates, Inc., 2019. http://papers.neurips.cc/paper/9015-pytorch-an-imperative-style-high-performance-deep-learning-library.pdf.

[159] M. Abadi, A. Agarwal, P. Barham, E. Brevdo, Z. Chen, C. Citro, G. S. Corrado, A. Davis, J. Dean, M. Devin, S. Ghemawat, I. Goodfellow, A. Harp, G. Irving, M. Isard, Y. Jia, R. Jozefowicz, L. Kaiser, M. Kudlur, J. Levenberg, D. Mané, R. Monga, S. Moore, D. Murray, C. Olah, M. Schuster, J. Shlens, B. Steiner, I. Sutskever, K. Talwar, P. Tucker, V. Vanhoucke, V. Vasudevan, F. Viégas, O. Vinyals, P. Warden, M. Wattenberg, M. Wicke, Y. Yu, and X. Zheng, "TensorFlow: Large-scale machine learning on heterogeneous systems," 2015. https://www.tensorflow.org/. Software available from tensorflow.org.

[160] J. Bradbury, R. Frostig, P. Hawkins, M. J. Johnson, C. Leary, D. Maclaurin, and S. Wanderman-Milne, "JAX: composable transformations of Python+NumPy programs," 2018. http://github.com/google/jax.

[161] S. S. Wilks, "The large-sample distribution of the likelihood ratio for testing composite hypotheses," *Ann. Math. Statist.* **9** no. 1, (03, 1938) 60–62. https://doi.org/10.1214/aoms/1177732360.

[162] A. Wald, "Tests of statistical hypotheses concerning several parameters when the number of observations is large," *Transactions of the American Mathematical Society* **54** no. 3, (1943) 426–482. https://doi.org/10.1090/S0002-9947-1943-0012401-3.

[163] G. Cowan, "Statistics for Searches at the LHC," in *69th Scottish Universities Summer School in Physics: LHC Physics*, pp. 321–355. 7, 2013. arXiv:1307.2487 [hep-ex].

[164] A. L. Read, "Presentation of search results: the CL_S technique," *J. Phys. G* **28** (2002) 2693.

[165] R. D. Cousins, J. T. Linnemann, and J. Tucker, "Evaluation of three methods for calculating statistical significance when incorporating a systematic uncertainty into a test of the background-only hypothesis for a Poisson process," *Nucl. Instrum. Meth. A* **595** no. 2, (2008) 480, arXiv:physics/0702156 [physics.data-an].

[166] K. CRANMER, "Statistical challenges for searches for new physics at the lhc," *Statistical Problems in Particle Physics, Astrophysics and Cosmology* (May, 2006) . http://dx.doi.org/10.1142/9781860948985_0026.

[167] ATLAS Collaboration, "Search for direct pair production of a chargino and a neutralino decaying to the 125 GeV Higgs boson in $\sqrt{s} = 8$ TeV pp collisions with the ATLAS detector," *Eur. Phys. J. C* **75** (2015) 208, arXiv:1501.07110 [hep-ex].

[168] ATLAS Collaboration, "Search for chargino and neutralino production in final states with a Higgs boson and missing transverse momentum at $\sqrt{s} = 13$ TeV with the ATLAS detector," *Phys. Rev. D* **100** (2019) 012006, arXiv:1812.09432 [hep-ex].

[169] CMS Collaboration, "Search for electroweak production of charginos and neutralinos in WH events in proton–proton collisions at $\sqrt{s} = 13$ TeV," *JHEP* **11** (2017) 029, arXiv:1706.09933 [hep-ex].

[170] ATLAS Collaboration, "Search for direct production of electroweakinos in final states with one lepton, missing transverse momentum and a Higgs boson decaying into two b-jets in pp collisions at $\sqrt{s} = 13$ TeV with the ATLAS detector," *Eur. Phys. J. C* **80** (2020) 691, arXiv:1909.09226 [hep-ex].

[171] ATLAS Collaboration, "Improvements in $t\bar{t}$ modelling using NLO+PS Monte Carlo generators for Run 2." ATL-PHYS-PUB-2018-009, 2018. https://cds.cern.ch/record/2630327.

[172] ATLAS Collaboration, "Modelling of the $t\bar{t}H$ and $t\bar{t}V(V = W, Z)$ processes for $\sqrt{s} = 13$ TeV ATLAS analyses." ATL-PHYS-PUB-2016-005, 2016. https://cds.cern.ch/record/2120826.

[173] ATLAS Collaboration, "ATLAS simulation of boson plus jets processes in Run 2." ATL-PHYS-PUB-2017-006, 2017. https://cds.cern.ch/record/2261937.

[174] ATLAS Collaboration, "Multi-Boson Simulation for 13 TeV ATLAS Analyses." ATL-PHYS-PUB-2017-005, 2017. https://cds.cern.ch/record/2261933.

[175] J. Alwall, R. Frederix, S. Frixione, V. Hirschi, F. Maltoni, O. Mattelaer, H. S. Shao, T. Stelzer, P. Torrielli, and M. Zaro, "The automated computation of tree-level and next-to-leading order differential cross sections, and their matching to parton shower simulations," *JHEP* **07** (2014) 079, arXiv:1405.0301 [hep-ph].

[176] R. Frederix and S. Frixione, "Merging meets matching in MC@NLO," *JHEP* **12** (2012) 061, arXiv:1209.6215 [hep-ph].

[177] T. Sjöstrand, S. Ask, J. R. Christiansen, R. Corke, N. Desai, P. Ilten, S. Mrenna, S. Prestel, C. O. Rasmussen, and P. Z. Skands, "An Introduction to PYTHIA 8.2," *Comput. Phys. Commun.* **191** (2015) 159–177, arXiv:1410.3012 [hep-ph].

[178] L. Lönnblad and S. Prestel, "Matching tree-level matrix elements with interleaved showers," *JHEP* **03** (2012) 019, arXiv:1109.4829 [hep-ph].

[179] R. D. Ball *et al.*, "Parton distributions with LHC data," *Nucl. Phys. B* **867** (2013) 244, arXiv:1207.1303 [hep-ph].

[180] ATLAS Collaboration, "ATLAS Pythia 8 tunes to 7 TeV data." ATL-PHYS-PUB-2014-021, 2014. https://cds.cern.ch/record/1966419.

[181] D. J. Lange, "The EvtGen particle decay simulation package," *Nucl. Instrum. Meth. A* **462** (2001) 152.

[182] ATLAS Collaboration, "The Pythia 8 A3 tune description of ATLAS minimum bias and inelastic measurements incorporating the Donnachie–Landshoff diffractive model." ATL-PHYS-PUB-2016-017, 2016. https://cds.cern.ch/record/2206965.

[183] B. Fuks, M. Klasen, D. R. Lamprea, and M. Rothering, "Precision predictions for electroweak superpartner production at hadron colliders with RESUMMINO," *Eur. Phys. J. C* **73** (2013) 2480, arXiv:1304.0790 [hep-ph].

[184] J. Fiaschi and M. Klasen, "Neutralino-chargino pair production at NLO+NLL with resummation-improved parton density functions for LHC Run II," *Phys. Rev. D* **98** no. 5, (2018) 055014, arXiv:1805.11322 [hep-ph].

[185] B. Fuks, M. Klasen, D. R. Lamprea, and M. Rothering, "Gaugino production in proton-proton collisions at a center-of-mass energy of 8 TeV," *JHEP* **10** (2012) 081, arXiv:1207.2159 [hep-ph].

[186] S. Alioli, P. Nason, C. Oleari, and E. Re, "A general framework for implementing NLO calculations in shower Monte Carlo programs: the POWHEG BOX," *JHEP* **06** (2010) 043, arXiv:1002.2581 [hep-ph].

[187] S. Frixione, P. Nason, and G. Ridolfi, "A Positive-weight next-to-leading-order Monte Carlo for heavy flavour hadroproduction," *JHEP* **09** (2007) 126, arXiv:0707.3088 [hep-ph].

[188] P. Nason, "A New method for combining NLO QCD with shower Monte Carlo algorithms," *JHEP* **11** (2004) 040, arXiv:hep-ph/0409146.

[189] E. Bothmann *et al.*, "Event generation with Sherpa 2.2," *SciPost Phys.* **7** no. 3, (2019) 034, arXiv:1905.09127 [hep-ph].

[190] S. Höche, F. Krauss, S. Schumann, and F. Siegert, "QCD matrix elements and truncated showers," *JHEP* **05** (2009) 053, arXiv:0903.1219 [hep-ph].

[191] S. Höche, F. Krauss, M. Schönherr, and F. Siegert, "QCD matrix elements + parton showers. The NLO case," *JHEP* **04** (2013) 027, arXiv:1207.5030 [hep-ph].

[192] **NNPDF** Collaboration, R. D. Ball *et al.*, "Parton distributions for the LHC run II," *JHEP* **04** (2015) 040, arXiv:1410.8849 [hep-ph].

[193] ATLAS Collaboration, "Example ATLAS tunes of Pythia8, Pythia6 and Powheg to an observable sensitive to Z boson transverse momentum." ATL-PHYS-PUB-2013-017, 2013. https://cds.cern.ch/record/1629317.

[194] M. Czakon and A. Mitov, "Top++: A program for the calculation of the top-pair cross-section at hadron colliders," *Comput. Phys. Commun.* **185** (2014) 2930, arXiv:1112.5675 [hep-ph].

[195] M. Cacciari, M. Czakon, M. Mangano, A. Mitov, and P. Nason, "Top-pair production at hadron colliders with next-to-next-to-leading logarithmic soft-gluon resummation," *Phys. Lett. B* **710** (2012) 612–622, arXiv:1111.5869 [hep-ph].

[196] P. Kant, O. M. Kind, T. Kintscher, T. Lohse, T. Martini, S. Mölbitz, P. Rieck, and P. Uwer, "HatHor for single top-quark production: Updated predictions and uncertainty estimates for single top-quark production in hadronic collisions," *Comput. Phys. Commun.* **191** (2015) 74–89, arXiv:1406.4403 [hep-ph].

[197] N. Kidonakis, "Two-loop soft anomalous dimensions for single top quark associated production with a W^- or H^-," *Phys. Rev. D* **82** (2010) 054018, arXiv:1005.4451 [hep-ph].

[198] J. M. Campbell and R. K. Ellis, "$t\bar{t}W^{+-}$ production and decay at NLO," *JHEP* **07** (2012) 052, arXiv:1204.5678 [hep-ph].

[199] A. Lazopoulos, T. McElmurry, K. Melnikov, and F. Petriello, "Next-to-leading order QCD corrections to $t\bar{t}Z$ production at the LHC," *Phys. Lett. B* **666** (2008) 62–65, arXiv:0804.2220 [hep-ph].

[200] R. Gavin, Y. Li, F. Petriello, and S. Quackenbush, "FEWZ 2.0: A code for hadronic Z production at next-to-next-to-leading order," arXiv:1011.3540 [hep-ph].

[201] **LHC Higgs Cross Section Working Group** Collaboration, D. de Florian *et al.*, "Handbook of LHC Higgs Cross Sections: 4. Deciphering the Nature of the Higgs Sector," arXiv:1610.07922 [hep-ph].

[202] ATLAS Collaboration, "Performance of the ATLAS track reconstruction algorithms in dense environments in LHC Run 2," *Eur. Phys. J. C* **77** (2017) 673, arXiv:1704.07983 [hep-ex].

[203] R. Frühwirth, "Application of Kalman filtering to track and vertex fitting," *Nucl. Instrum. Methods Phys. Res., A* **262** no. HEPHY-PUB-503, (Jun, 1987) 444. 19 p. https://cds.cern.ch/record/178627.

[204] T. Cornelissen, M. Elsing, I. Gavrilenko, W. Liebig, E. Moyse, and A. Salzburger, "The new ATLAS track reconstruction (NEWT)," *J. Phys.: Conf. Ser.* **119** (2008) 032014. https://cds.cern.ch/record/1176900.

[205] ATLAS Collaboration, "Vertex Reconstruction Performance of the ATLAS Detector at $\sqrt{s} = 13$ TeV." ATL-PHYS-PUB-2015-026, 2015. https://cds.cern.ch/record/2037717.

[206] ATLAS Collaboration, "Reconstruction of primary vertices at the ATLAS experiment in Run 1 proton–proton collisions at the LHC," *Eur. Phys. J. C* **77** (2017) 332, arXiv:1611.10235 [hep-ex].

[207] ATLAS Collaboration, "Topological cell clustering in the ATLAS calorimeters and its performance in LHC Run 1," *Eur. Phys. J. C* **77** (2017) 490, arXiv:1603.02934 [hep-ex].

[208] ATLAS Collaboration, "Electron and photon performance measurements with the ATLAS detector using the 2015–2017 LHC proton–proton collision data," *JINST* **14** (2019) P12006, arXiv:1908.00005 [hep-ex].

[209] ATLAS Collaboration, "Measurement of the photon identification efficiencies with the ATLAS detector using LHC Run 2 data collected in 2015 and 2016," *Eur. Phys. J. C* **79** (2019) 205, arXiv:1810.05087 [hep-ex].

[210] ATLAS Collaboration, "Electron reconstruction and identification in the ATLAS experiment using the 2015 and 2016 LHC proton–proton collision data at $\sqrt{s} = 13$ TeV," *Eur. Phys. J. C* **79** (2019) 639, arXiv:1902.04655 [hep-ex].

[211] ATLAS Collaboration, "Muon reconstruction performance of the ATLAS detector in proton–proton collision data at $\sqrt{s} = 13$ TeV," *Eur. Phys. J. C* **76** (2016) 292, arXiv:1603.05598 [hep-ex].

[212] **ATLAS** Collaboration, "Muon reconstruction and identification efficiency in ATLAS using the full Run 2 *pp* collision data set at $\sqrt{s} = 13$ TeV," arXiv:2012.00578 [hep-ex].

[213] M. Cacciari, G. P. Salam, and G. Soyez, "The anti-k_t jet clustering algorithm," *JHEP* **04** (2008) 063, arXiv:0802.1189 [hep-ph].

[214] M. Cacciari, G. P. Salam, and G. Soyez, "FastJet user manual," *Eur. Phys. J. C* **72** (2012) 1896, arXiv:1111.6097 [hep-ph].

[215] M. Cacciari, "FastJet: A Code for fast k_t clustering, and more," in *Deep inelastic scattering. Proceedings, 14th International Workshop, DIS 2006, Tsukuba, Japan, April 20-24, 2006*, pp. 487–490. 2006. arXiv:hep-ph/0607071 [hep-ph]. [,125(2006)].

[216] **ATLAS** Collaboration, G. Aad *et al.*, "Jet energy scale and resolution measured in proton-proton collisions at $\sqrt{s} = 13$ TeV with the ATLAS detector," arXiv:2007.02645 [hep-ex].

[217] M. Cacciari and G. P. Salam, "Pileup subtraction using jet areas," *Phys. Lett. B* **659** (2008) 119–126, arXiv:0707.1378 [hep-ph].

[218] ATLAS Collaboration, "Jet energy measurement with the ATLAS detector in proton–proton collisions at $\sqrt{s} = 7$ TeV," *Eur. Phys. J. C* **73** (2013) 2304, arXiv:1112.6426 [hep-ex].

[219] ATLAS Collaboration, "Determination of jet calibration and energy resolution in proton–proton collisions at $\sqrt{s} = 8$ TeV using the ATLAS detector," arXiv:1910.04482 [hep-ex].

[220] ATLAS Collaboration, "Performance of pile-up mitigation techniques for jets in *pp* collisions at $\sqrt{s} = 8$ TeV using the ATLAS detector," *Eur. Phys. J. C* **76** (2016) 581, arXiv:1510.03823 [hep-ex].

[221] ATLAS Collaboration, "Optimisation and performance studies of the ATLAS *b*-tagging algorithms for the 2017-18 LHC run." ATL-PHYS-PUB-2017-013, 2017. https://cds.cern.ch/record/2273281.

[222] ATLAS Collaboration, "ATLAS b-jet identification performance and efficiency measurement with $t\bar{t}$ events in pp collisions at $\sqrt{s} = 13\,\text{TeV}$," *Eur. Phys. J. C* **79** (2019) 970, arXiv:1907.05120 [hep-ex].

[223] ATLAS Collaboration, "Measurements of b-jet tagging efficiency with the ATLAS detector using $t\bar{t}$ events at $\sqrt{s} = 13\,\text{TeV}$," *JHEP* **08** (2018) 089, arXiv:1805.01845 [hep-ex].

[224] ATLAS Collaboration, "Performance of missing transverse momentum reconstruction with the ATLAS detector using proton–proton collisions at $\sqrt{s} = 13\,\text{TeV}$," *Eur. Phys. J. C* **78** (2018) 903, arXiv:1802.08168 [hep-ex].

[225] **ATLAS Collaboration** Collaboration, "$E_{\text{T}}^{\text{miss}}$ performance in the ATLAS detector using 2015-2016 LHC p-p collisions," Tech. Rep. ATLAS-CONF-2018-023, CERN, Geneva, Jun, 2018. http://cds.cern.ch/record/2625233.

[226] D. Adams *et al.*, "Recommendations of the Physics Objects and Analysis Harmonisation Study Groups 2014," Tech. Rep. ATL-PHYS-INT-2014-018, CERN, Geneva, Jul, 2014. https://cds.cern.ch/record/1743654.

[227] M. Cacciari, G. P. Salam, and G. Soyez, "The Catchment Area of Jets," *JHEP* **04** (2008) 005, arXiv:0802.1188 [hep-ph].

[228] **UA1** Collaboration, G. Arnison *et al.*, "Experimental Observation of Isolated Large Transverse Energy Electrons with Associated Missing Energy at $\sqrt{s} = 540$ GeV," *Phys. Lett. B* **122** (1983) 103–116.

[229] **Aachen-Annecy-Birmingham-CERN-Helsinki-London(QMC)-Paris(CdF)-Riverside-Rome-Rutherford-Saclay(CEN)-Vienna** Collaboration, G. Arnison *et al.*, "Further evidence for charged intermediate vector bosons at the SPS collider," *Phys. Lett. B* **129** no. CERN-EP-83-111, (Jun, 1985) 273–282. 17 p. https://cds.cern.ch/record/163856.

[230] D. R. Tovey, "On measuring the masses of pair-produced semi-invisibly decaying particles at hadron colliders," *JHEP* **04** (2008) 034, arXiv:0802.2879 [hep-ph].

[231] G. Polesello and D. R. Tovey, "Supersymmetric particle mass measurement with the boost-corrected contransverse mass," *JHEP* **03** (2010) 030, arXiv:0910.0174 [hep-ph].

[232] **ATLAS** Collaboration, G. Aad *et al.*, "Performance of the missing transverse momentum triggers for the ATLAS detector during Run-2 data taking," *JHEP* **08** (2020) 080, arXiv:2005.09554 [hep-ex].

[233] **ATLAS** Collaboration, G. Aad *et al.*, "Performance of algorithms that reconstruct missing transverse momentum in $\sqrt{s} = 8$ TeV proton-proton collisions in the ATLAS detector," *Eur. Phys. J. C* **77** no. 4, (2017) 241, arXiv:1609.09324 [hep-ex].

[234] ATLAS Collaboration, "ATLAS data quality operations and performance for 2015–2018 data-taking," *JINST* **15** (2020) P04003, arXiv:1911.04632 [physics.ins-det].

[235] ATLAS Collaboration, "Selection of jets produced in 13 TeV proton–proton collisions with the ATLAS detector." ATLAS-CONF-2015-029, 2015. https://cds.cern.ch/record/2037702.

[236] N. Hartmann, "ahoi." https://gitlab.com/nikoladze/ahoi, 2018.

[237] **ATLAS** Collaboration, "Object-based missing transverse momentum significance in the ATLAS detector," Tech. Rep. ATLAS-CONF-2018-038, CERN, Geneva, Jul, 2018. https://cds.cern.ch/record/2630948.

[238] A. Roodman, "Blind analysis in particle physics," *eConf* **C030908** (2003) TUIT001, arXiv:physics/0312102.

[239] ATLAS Collaboration, "A method for the construction of strongly reduced representations of ATLAS experimental uncertainties and the application thereof to the jet energy scale." ATL-PHYS-PUB-2015-014, 2015. https://cds.cern.ch/record/2037436.

[240] J. Bellm *et al.*, "Herwig 7.0/Herwig++ 3.0 release note," *Eur. Phys. J.* **C76** no. 4, (2016) 196, arXiv:1512.01178 [hep-ph].

[241] ATLAS Collaboration, "Simulation of top-quark production for the ATLAS experiment at $\sqrt{s} = 13$ TeV." ATL-PHYS-PUB-2016-004, 2016. https://cds.cern.ch/record/2120417.

[242] S. Frixione, E. Laenen, P. Motylinski, C. White, and B. R. Webber, "Single-top hadroproduction in association with a W boson," *JHEP* **07** (2008) 029, arXiv:0805.3067 [hep-ph].

[243] **ATLAS Collaboration** Collaboration, "SUSY July 2020 Summary Plot Update," Tech. Rep. ATL-PHYS-PUB-2020-020, CERN, Geneva, Jul, 2020. http://cds.cern.ch/record/2725258.

[244] G. Apollinari, I. Béjar Alonso, O. Brüning, M. Lamont, and L. Rossi, *High-Luminosity Large Hadron Collider (HL-LHC): Preliminary Design Report*. CERN Yellow Reports: Monographs. CERN, Geneva, 2015. https://cds.cern.ch/record/2116337.

[245] **LHC Reinterpretation Forum** Collaboration, W. Abdallah *et al.*, "Reinterpretation of LHC Results for New Physics: Status and Recommendations after Run 2," *SciPost Phys.* **9** no. 2, (2020) 022, arXiv:2003.07868 [hep-ph].

[246] ATLAS Collaboration, "RECAST framework reinterpretation of an ATLAS Dark Matter Search constraining a model of a dark Higgs boson decaying to two b-quarks." ATL-PHYS-PUB-2019-032, 2019. https://cds.cern.ch/record/2686290.

[247] K. Cranmer and I. Yavin, "RECAST: Extending the Impact of Existing Analyses," *JHEP* **04** (2011) 038, arXiv:1010.2506 [hep-ex].

[248] S. Ovyn, X. Rouby, and V. Lemaitre, "DELPHES, a framework for fast simulation of a generic collider experiment," arXiv:0903.2225 [hep-ph].

[249] A. Buckley, J. Butterworth, D. Grellscheid, H. Hoeth, L. Lonnblad, J. Monk, H. Schulz, and F. Siegert, "Rivet user manual," *Comput. Phys. Commun.* **184** (2013) 2803–2819, arXiv:1003.0694 [hep-ph].

[250] A. Buckley, D. Kar, and K. Nordström, "Fast simulation of detector effects in Rivet," *SciPost Phys.* **8** (2020) 025, arXiv:1910.01637 [hep-ph].

[251] D. Dercks, N. Desai, J. S. Kim, K. Rolbiecki, J. Tattersall, and T. Weber, "CheckMATE 2: From the model to the limit," *Comput. Phys. Commun.* **221** (2017) 383–418, arXiv:1611.09856 [hep-ph].

[252] M. Drees, H. Dreiner, D. Schmeier, J. Tattersall, and J. S. Kim, "CheckMATE: Confronting your Favourite New Physics Model with LHC Data," *Comput. Phys. Commun.* **187** (2015) 227–265, arXiv:1312.2591 [hep-ph].

[253] E. Conte, B. Fuks, and G. Serret, "MadAnalysis 5, A User-Friendly Framework for Collider Phenomenology," *Comput. Phys. Commun.* **184** (2013) 222–256, arXiv:1206.1599 [hep-ph].

[254] E. Maguire, L. Heinrich, and G. Watt, "HEPData: a repository for high energy physics data," *J. Phys. Conf. Ser.* **898** no. 10, (2017) 102006, arXiv:1704.05473 [hep-ex].

[255] **ATLAS** Collaboration, "Simpleanalysis." https://gitlab.cern.ch/atlas-sa/simple-analysis, 2021.

[256] S. Kraml, S. Kulkarni, U. Laa, A. Lessa, W. Magerl, D. Proschofsky-Spindler, and W. Waltenberger, "SModelS: a tool for interpreting simplified-model results from the LHC and its application to supersymmetry," *Eur. Phys. J. C* **74** (2014) 2868, arXiv:1312.4175 [hep-ph].

[257] F. Ambrogi, S. Kraml, S. Kulkarni, U. Laa, A. Lessa, V. Magerl, J. Sonneveld, M. Traub, and W. Waltenberger, "SModelS v1.1 user manual: Improving simplified model constraints with efficiency maps," *Comput. Phys. Commun.* **227** (2018) 72–98, arXiv:1701.06586 [hep-ph].

[258] **ATLAS** Collaboration, "Search for direct production of electroweakinos in final states with one lepton, missing transverse momentum and a higgs boson decaying into two b-jets in pp collisions at $\sqrt{s} = 13$ tev with the atlas detector," 2021. https://www.hepdata.net/record/ins1755298?version=4.

[259] **LHC Reinterpretation Forum** Collaboration, W. Abdallah *et al.*, "Reinterpretation of LHC Results for New Physics: Status and Recommendations after Run 2," *SciPost Phys.* **9** no. 2, (2020) 022, arXiv:2003.07868 [hep-ph].

[260] **ATLAS** Collaboration, "1lbb-likelihoods-hepdata.tar.gz," 2020. https://www.hepdata.net/record/resource/1408476?view=true.

[261] G. Alguero, S. Kraml, and W. Waltenberger, "A SModelS interface for pyhf likelihoods," arXiv:2009.01809 [hep-ph].

[262] M. D. Goodsell, "Implementation of the ATLAS-SUSY-2019-08 analysis in the MadAnalysis 5 framework (electroweakinos with a Higgs decay into a $b\bar{b}$ pair, one lepton and missing transverse energy; 139 fb^{-1})," *Mod. Phys. Lett. A* **36** no. 01, (2021) 2141006.

[263] J. Y. Araz *et al.*, "Proceedings of the second MadAnalysis 5 workshop on LHC recasting in Korea," *Mod. Phys. Lett. A* **36** no. 01, (2021) 2102001, arXiv:2101.02245 [hep-ph].

[264] M. Feickert, L. Heinrich, G. Stark, and B. Galewsky, "Distributed statistical inference with pyhf enabled through funcX," in *25th International Conference on Computing in High-Energy and Nuclear Physics*. 3, 2021. arXiv:2103.02182 [cs.DC].

[265] R. Chard, Y. Babuji, Z. Li, T. Skluzacek, A. Woodard, B. Blaiszik, I. Foster, and K. Chard, "funcx: A federated function serving fabric for science," ACM, Jun, 2020. http://dx.doi.org/10.1145/3369583.3392683.

[266] D. Merkel, "Docker: Lightweight linux containers for consistent development and deployment," *Linux J.* **2014** no. 239, (Mar., 2014) .

[267] S. Binet and B. Couturier, "docker & HEP: Containerization of applications for development, distribution and preservation," *J. Phys.: Conf. Ser.* **664** no. 2, (2015) 022007. 8 p. https://cds.cern.ch/record/2134524.

[268] K. Cranmer and L. Heinrich, "Yadage and Packtivity - analysis preservation using parametrized workflows," *J. Phys. Conf. Ser.* **898** no. 10, (2017) 102019, arXiv:1706.01878 [physics.data-an].

[269] ATLAS Collaboration, "Summary of the ATLAS experiment's sensitivity to supersymmetry after LHC Run 1 — interpreted in the phenomenological MSSM," *JHEP* **10** (2015) 134, arXiv:1508.06608 [hep-ex].

[270] ATLAS Collaboration, "Searches for electroweak production of supersymmetric particles with compressed mass spectra in $\sqrt{s} = 13\,\text{TeV}$ pp collisions with the ATLAS detector," *Phys. Rev. D* **101** (2020) 052005, arXiv:1911.12606 [hep-ex].

[271] ATLAS Collaboration, "Search for electroweak production of charginos and sleptons decaying into final states with two leptons and missing transverse momentum in $\sqrt{s} = 13\,\text{TeV}$ pp collisions using the ATLAS detector," *Eur. Phys. J. C* **80** (2020) 123, arXiv:1908.08215 [hep-ex].

[272] ATLAS Collaboration, "Search for direct stau production in events with two hadronic τ-leptons in $\sqrt{s} = 13\,\text{TeV}$ pp collisions with the ATLAS detector," *Phys. Rev. D* **101** (2020) 032009, arXiv:1911.06660 [hep-ex].

[273] ATLAS Collaboration, "Search for bottom-squark pair production with the ATLAS detector in final states containing Higgs bosons, b-jets and missing transverse momentum," *JHEP* **12** (2019) 060, arXiv:1908.03122 [hep-ex].

[274] W. Porod, "SPheno, a program for calculating supersymmetric spectra, SUSY particle decays and SUSY particle production at e+ e- colliders," *Comput. Phys. Commun.* **153** (2003) 275–315, arXiv:hep-ph/0301101.

[275] W. Porod and F. Staub, "SPheno 3.1: Extensions including flavour, CP-phases and models beyond the MSSM," *Comput. Phys. Commun.* **183** (2012) 2458–2469, arXiv:1104.1573 [hep-ph].

[276] S. Heinemeyer, W. Hollik, and G. Weiglein, "FeynHiggs: A Program for the calculation of the masses of the neutral CP even Higgs bosons in the MSSM," *Comput. Phys. Commun.* **124** (2000) 76–89, arXiv:hep-ph/9812320.

[277] H. Bahl, T. Hahn, S. Heinemeyer, W. Hollik, S. Paßehr, H. Rzehak, and G. Weiglein, "Precision calculations in the MSSM Higgs-boson sector with FeynHiggs 2.14," *Comput. Phys. Commun.* **249** (2020) 107099, arXiv:1811.09073 [hep-ph].

[278] T. Hahn, S. Heinemeyer, W. Hollik, H. Rzehak, and G. Weiglein, "High-Precision Predictions for the Light CP -Even Higgs Boson Mass of the Minimal Supersymmetric Standard Model," *Phys. Rev. Lett.* **112** no. 14, (2014) 141801, arXiv:1312.4937 [hep-ph].

[279] B. C. Allanach, "SOFTSUSY: a program for calculating supersymmetric spectra," *Comput. Phys. Commun.* **143** (2002) 305–331, arXiv:hep-ph/0104145 [hep-ph].

[280] G. Belanger, F. Boudjema, A. Pukhov, and A. Semenov, "MicrOMEGAs 2.0: A Program to calculate the relic density of dark matter in a generic model," *Comput. Phys. Commun.* **176** (2007) 367–382, arXiv:hep-ph/0607059.

[281] G. Belanger, F. Boudjema, A. Pukhov, and A. Semenov, "micrOMEGAs: A Tool for dark matter studies," *Nuovo Cim. C* **033N2** (2010) 111–116, arXiv:1005.4133 [hep-ph].

[282] F. Mahmoudi, "SuperIso v2.3: A Program for calculating flavor physics observables in Supersymmetry," *Comput. Phys. Commun.* **180** (2009) 1579–1613, arXiv:0808.3144 [hep-ph].

[283] W. Beenakker, R. Hopker, and M. Spira, "PROSPINO: A Program for the Production of Supersymmetric Particles in Next-to-leading Order QCD," Tech. Rep. hep-ph/9611232, Nov, 1996. https://cds.cern.ch/record/314229. 12 pages, latex, no figures, Complete postscript file and FORTRAN source codes available from http://wwwcn.cern.ch/ mspira/prospino/.

[284] W. Beenakker, M. Klasen, M. Kramer, T. Plehn, M. Spira, and P. M. Zerwas, "The Production of charginos / neutralinos and sleptons at hadron colliders," *Phys. Rev. Lett.* **83** (1999) 3780–3783, arXiv:hep-ph/9906298. [Erratum: Phys.Rev.Lett. 100, 029901 (2008)].

[285] A. Arbey, M. Battaglia, and F. Mahmoudi, "Higgs Production in Neutralino Decays in the MSSM - The LHC and a Future e^+e^- Collider," *Eur. Phys. J. C* **75** no. 3, (2015) 108, arXiv:1212.6865 [hep-ph].

[286] M. E. Cabrera, J. A. Casas, A. Delgado, S. Robles, and R. Ruiz de Austri, "Naturalness of MSSM dark matter," *JHEP* **08** (2016) 058, arXiv:1604.02102 [hep-ph].